The Thesis Committee for Kyle Austin Wright
Certifies that this is the approved version of the following thesis:

Hydrological connectivity in vegetated river deltas: the effects of spatial variability and patchiness on channel-island exchange

APPROVED BY
SUPERVISING COMMITTEE:

Paola Passalacqua, Supervisor

David Mohrig

Hydrological connectivity in vegetated river deltas: the effects of spatial variability and patchiness on channel-island exchange

by

Kyle Austin Wright

Thesis

Presented to the Faculty of the Graduate School of

The University of Texas at Austin

in Partial Fulfillment

of the Requirements

for the Degree of

Master of Science in Engineering

The University of Texas at Austin

May 2018

Acknowledgments

First and foremost, I would like to thank my advisor, Dr. Paola Passalacqua, without whom none of this would have been possible. This project started because of a chance you took in inviting me to do undergraduate research with your team, and everything since has been largely a result of that. It has been a pleasure working with such a brilliant, inspirational, and friendly advisor, and I look forward to continuing to do so. I would also like to thank Dr. Matt Hiatt, for mentoring me as an undergrad and allowing me to be a part of the continuation and evolution of this project. I am a person who learns best by example, and I cannot imagine having had a better example. In addition, I thank Dr. Desmond Lawler, Dr. Ben Hodges, Dr. Charles Werth, and Dr. Richard Corsi for teaching me to love environmental engineering, for encouraging me to go to grad school, and for all of the countless lessons they have provided me.

I would like to thank Alicia Sendrowski, Jeff Zheng, Lukas Godbout, Tess Jarriel, and the teams of Dr. David Mohrig and Dr. Wonsuck Kim for their guidance, friendship, and feedback on this research over the past two years. I thank Dr. Heidi Nepf, for providing very useful comments at the onset of this project. I thank my friends Alex Reidel, John Ramos, and Evan Reidel, for being the greatest friends imaginable. And I thank my girlfriend Mickey Lanning for her unwavering support, and for not only listening to me ramble about this research, but for doing so enthusiastically. I am astoundingly lucky to have had all of these people in my life.

I acknowledge the funding support of the National Science Foundation Graduate Research Fellowship (grant DGE-1610403) and the Cockrell School of Engineering at UT Austin. This research has been additionally supported by NSF grants CAREER/EAR-1350336 and FESD/EAR-1135427 awarded to Dr. Passalacqua, the NSF GRFP under grant DGE-1110007 awarded to Dr. Hiatt.

Hydrological connectivity in vegetated river deltas: the effects of spatial variability and patchiness on channel-island exchange

by

Kyle Austin Wright, M.S.E.
The University of Texas at Austin, 2018
Supervisor: Paola Passalacqua

River deltas are threatened regions of great societal and environmental importance, and their continued survival depends upon a greater understanding of their formation and evolution. Hydrological connectivity in river deltas is important for delivering flow and sediment to the island interior and is responsible for a large portion of the ecosystem benefits that deltas provide, which could be leveraged for restoration projects using nature-based engineering. However, the process is still poorly understood. The roughness of island vegetation is known to significantly limit channel-island connectivity, but the importance of the spatial distribution of vegetation is, as-of-yet, unknown. Using a 2D hydrodynamic model, we investigate the influence of vegetation percent cover, patch size, and stem density on the fraction of discharge allocated to the islands of an idealized delta complex, modeled after the Wax Lake Delta in coastal Louisiana. We find that spatial heterogeneity can substantially alter connectivity when vegetation is dense and covers less than a "disconnectivity" threshold near 50% of the island domain, near

the theoretical percolation limit. Above this threshold, models can accurately approximate vegetation as uniform. Below this threshold, however, preferential flow-paths develop in the islands, which greatly alter the hydraulics, transport capabilities, and residence time distribution of the delta complex, with respect to what is seen in uniform vegetation cases. Our results suggest that patchiness has substantial hydrogeomorphic and biogeochemical implications which should be considered when modeling deltaic systems.

Table of Contents

List of Tables

List of Figures

Chapter 1: Introduction

1.1 Deltaic systems: socioeconomic importance and threats

Coastal river deltas are regions of tremendous societal and ecological importance. They are home to hundreds of millions of people worldwide [*McGranahan et al.*, 2007; *Tessler et al.*, 2015], and many are huge hubs of economic activity — more than half of the global GDP is generated within the coastal zone, primarily within heavily populated delta regions [*McGranahan et al.*, 2007; *Vörösmarty et al.*, 2009], and even conservative estimates place their worldwide economic value to be in the trillions of US dollars [*Giosan*, 2014]. The wetlands of river deltas provide a number of valuable ecosystem services, and are home to countless unique and ecologically diverse ecosystems [*Kingsford*, 2000; *Li et al.*, 2012]. Deltaic wetlands improve water quality by treating nutrients released upstream [*Hiatt et al.*, 2018], which would otherwise contribute to off-shore hypoxic zones, therefore acting as a natural buffer zone for nutrients. Deltas also act as blue Carbon sinks to an estimated 75 TgC per year [*Smith et al.*, 2015], with some deltas accumulating Carbon at a rate comparable to or greater than other blue Carbon habitats [*Shields et al.*, 2017].

Despite their significance, coastal deltas are predicted to be subject to increasingly high risks in the face of global environmental change; both natural and anthropogenic factors threaten the long-term sustainability of a majority of the world's major deltas [*Syvitski et al.*, 2009; *Tessler et al.*, 2015; *Day et al.*, 2016; *Tessler et al.*, 2017]. Worldwide, deltas are sinking into the sea at a record pace. Deltas naturally subside as new accumulated sediment consolidates, but many deltas are experiencing enhanced subsidence rates due to hydrocarbon extraction [*Morton et al.*, 2005; *Couvillion et al.*, 2011]. When combined with sea-level rise due to climate change, which is projected to be substantial over the next century

Text from this chapter has been submitted in an article to Geophysical Research Letters with Kyle Wright, Matthew Hiatt, and Paola Passalacqua as authors.

[*Nicholls and Cazenave*, 2010; *Grinsted et al.*, 2010], this leads to very high rates of relative sea-level rise in many coastal deltas [*Syvitski et al.*, 2009; *Tessler et al.*, 2017]. The location of coastal deltas leaves them particularly vulnerable to flood-induced erosion, as they not only have to face fluvial flooding, but also waves, storm surge, and winds induced by tropical cyclones [*Xing et al.*, 2017]. In many catchments around the globe, not only are large-intensity storms that cause fluvial flooding projected to increase under the changing climate [*Hirabayashi et al.*, 2013], but also the frequency of the largest tropical storms [*Knutson et al.*, 2010].

In addition to flooding and land loss threatening the physical deltaic system, the populations and ecosystems who depend on these systems for their livelihood are also threatened by pollution [*Mendelssohn et al.*, 2012; *Bai et al.*, 2012], hypoxia and eutrophication [*Mitsch et al.*, 2001; *Paola et al.*, 2011], and saltwater intrusion [*Zhang et al.*, 2012]. When combined with coastal flooding, each of these issues can work in concert to harm local economies, communities, and agriculture. It has also been shown that the human populations most vulnerable to these threats are typically those in the lowest socioeconomic class who most lack the resources to respond to floods or rising seas [*Adger*, 1999; *Douglas et al.*, 2008; *Donner and Rodríguez*, 2008]. While the loss of deltaic systems is an environmental and economic concern, it is additionally a problem of environmental justice, as these issues tend to enforce and exacerbate existing inequalities between populations along lines of race, gender, and class [*Donner and Rodríguez*, 2008].

Historically, engineering efforts have had a mixed effect on mitigating coastal flooding. The addition of flow control structures and levees alleviates flooding on the short-term, but on the long-term these projects have cut off the sediment supply to deltaic floodplains and wetlands and have contributed to the rapid land loss seen in many coastal areas (e.g. Figure 1.1 shows projected land loss in Louisiana over the next 50 years if no action is taken to mitigate, *CPRA* [2017]). In un-engineered deltas, sediment consolidation within the floodplains is naturally balanced by regular over-bank sediment deposition from the main channel [*Kim et al.*, 2009b]. The overconfinement of the riverine input has eliminated the channel-floodplain connectivity on which sustainable deltaic evolution depends [*Paola et al.*, 2011]. It is for this reason that the Louisiana coast has lost around $5000km^2$ of land over the past century despite continuing to deliver over $100Mt$ of

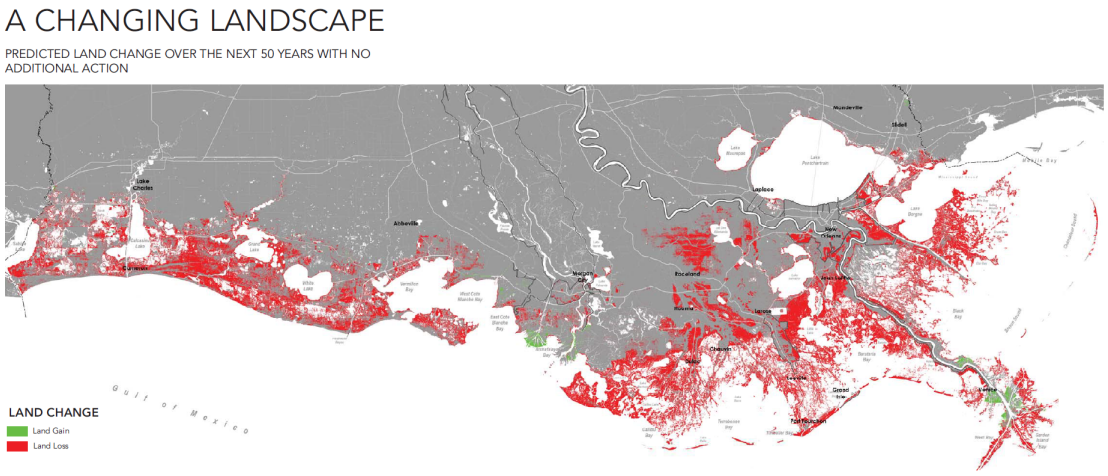

Figure 1.1: Projected land loss in coastal Louisiana over the next 50 years with no mitigation/restoration action. Figure from 2017 Master Plan for a Sustainable Coast [*CPRA*, 2017]

sediment to the coast every year [*Kim et al.*, 2009b; *Nittrouer and Viparelli*, 2014; *CPRA*, 2017]. When combined with the upstream construction of dams, which further reduce the load of suspended sediment delivered to the coast, the result is that many deltas have become sediment-starved [*Syvitski et al.*, 2005, 2009; *Paola et al.*, 2011; *Giosan*, 2014; *Auerbach et al.*, 2015]. In addition to altering the behavior of the physical deltaic system, these water management practices have also impacted the way populations interact with these systems [*Kingsford*, 2000; *Leauthaud et al.*, 2013].

1.2 Coastal restoration with nature-based engineering

Research in engineering projects which aim to restore river deltas or mitigate additional harm have seen a rapid increase in focus and funding in the past several decades [e.g. *Turner et al.*, 2007; *Kim et al.*, 2009b; *Paola et al.*, 2011; *Schmitt et al.*, 2013], and authorities in many locations have already invested large sums of money towards their implementation [*CPRA*, 2017]. The prevailing paradigm in coastal engineering has shifted in recent years, from the traditional approach which fought the dynamic behavior of deltas, to one which takes advantage of

the natural processes by which deltas self-maintain. This "ecosystem-based" or "nature-based" engineering aims to use natural processes to restore deltas and shield them against storm surges, nutrient overloading, and land loss [*Temmerman et al.*, 2013; *Giosan*, 2014; *Temmerman and Kirwan*, 2015].

A number of studies have demonstrated that expanding coastal wetlands can help mitigate flooding in the mainland by attenuating waves and storm surge associated with tropical storms [*Wamsley et al.*, 2010; *Shepard et al.*, 2011; *Barbier et al.*, 2013; *Leonardi et al.*, 2017]. For example, *Barbier et al.* [2013] found that a 1% increase in wetland roughness due to vegetation resulted in a 15%-28% decrease in storm surge, with avoided damages leading to considerable savings for residential property owners. Expanding wetlands has the additional benefit of increasing biogeochemical nutrient processing [*Mitsch et al.*, 2001, 2005; *Rivera-Monroy et al.*, 2013; *Cheng and Basu*, 2017]. The structure of macrophytic plants slows down flow, which allows miscroscopic organisms and algae (and to some extent the macrophytes themselves) to sequester Nitrogen, Phosphorus, and other pollutants from upstream agricultural and urban runoff [*Kadlec and Wallace*, 2008]. This can notably improve water quality and prevent the production and expansion of hypoxic zones.

Restoration projects that incorporate nature-based engineering principles typically fall into the categories of marsh expansion and sediment diversions. In coastal Louisiana, these two project types have been allocated $17.8 billion and $5.1 billion, respectively, which together make up almost 92% of the total spending allocated for restoration efforts [*CPRA*, 2017]. Nearly all of the land built or maintained due to restoration efforts is expected to come from one of these two project types. Sediment diversions are engineered breaches in levees that aim to reconnect fluvial sediment supplies to their sediment-starved floodplains [*Kim et al.*, 2009b], and despite each diversion only receiving a small fraction of the channel flow, they are projected to result in a majority of the new land built under the master plan [*CPRA*, 2017]. Reinstating this natural channel-floodplain or channel-island connectivity not only builds land by the deposition of fluvial sediment, but also rehabilitates wetlands, which for the aforementioned reasons further improves water quality and limits saltwater intrusion [*Lane et al.*, 2007; *Michot et al.*, 2015]. Once completed, these projects lessen a number of the threats

deltaic systems face, all while requiring minimal intervention on the part of humans — the system maintains itself.

A number of modeling efforts have been devoted to predicting the impact of these projects on deltaic systems [e.g. *Kim et al.*, 2009b; *Li et al.*, 2012; *Meselhe et al.*, 2012, 2013; *Wang et al.*, 2014; *Yuill et al.*, 2016]. However, these efforts are hindered by our current lack of understanding of the precise mechanisms by which deltas build land, evolve, and respond to environmental change, even in fully natural systems — let alone those perturbed by extensive anthropogenic modification.

1.3 Connectivity in river deltas

One of the central obstacles to obtaining a full understanding of deltaic systems is their high degree of complexity. Distributary networks tend to be very morphodynamically and topologically complex [*Tejedor et al.*, 2015a,b, 2016] and highly interconnected [*Hiatt and Passalacqua*, 2015; *Passalacqua*, 2017]. Much remains unknown about the structural and functional connections within the deltaic system, between landscape elements (e.g. channels and islands) as well as among system variables (e.g. vegetation, sediment, and flow).

Natural river deltas are "leaky networks" [*Passalacqua*, 2017] in which the distributary channels and interdistributary islands are hydrologically connected. In certain distributaries of the Wax Lake Delta in Louisiana, *Hiatt and Passalacqua* [2015] observed that up to 28%-54% of the channel flow is allocated to the interdistributary islands before being discharged into the bay under non-flood conditions — an observation that has since been backed up by other studies [*Liang et al.*, 2015; *Shaw et al.*, 2016b; *Hiatt and Passalacqua*, 2017; *Hiatt et al.*, 2018]. In addition, *Sendrowski and Passalacqua* [2017] revealed the existence of information transfer among system drivers (e.g. discharge, tides, and wind) and system variables (e.g. water level, nitrate concentrations) which spans the full delta complex, indicating that deltaic processes can be measurably affected by non-local interactions. Because deltaic islands are of central importance for land growth and ecosystem services (e.g. marsh creation, water quality improvements), the success of nature-based engineering projects depends upon our understanding of

channel-island connectivity, and to what degree it is influenced by system drivers.

One previous study, *Hiatt and Passalacqua* [2017], looked at the influence of discharge, tides, and island vegetative roughness on channel-island connectivity. Through hydrodynamic modeling, they found that discharge and tides do not have a notable effect on the percentage of channel flow allocated to the islands (when averaged over a tidal cycle) — but an increase in vegetative roughness is able to substantially limit connectivity. Model runs with higher vegetated roughness see an increase in the percentage of flow that remains confined, in addition to raised water surface elevations throughout the full backwater zone, diminished channel velocities just upstream of the onset of lateral outflow, and longer residence times in the islands. As such, the presence of island vegetation may be one of the most important factors influencing channel-island connectivity.

However, the numerical modeling done in *Hiatt and Passalacqua* [2017], as well as in other studies [e.g., *Nardin et al.*, 2016; *Hiatt et al.*, 2018], used the simplifying assumption that vegetation is spatially-uniform within the islands. While this may be a reasonable approximation, deltaic vegetation is often far from uniform (Figure 1.2). It has yet to be shown how more complex spatial-distributions of vegetation affect the degree of hydrological connectivity in a deltaic system. How does the spatial heterogeneity of vegetation affect connectivity? Under what circumstances can vegetation be approximated as uniform?

1.4 Ecogeomorphology in deltaic wetlands

It has been recognized for some time that heterogeneity can play an important role in flow and transport through a system. In the subsurface, rock fractures and differences in hydrologic conductivity can substantially impact groundwater fluxes and the transport of environmental pollutants [*Freeze*, 1975; *Dagan*, 1984; *Michael and Voss*, 2008; *Khan et al.*, 2016]. Several researchers have shown that vegetation could drive similar behavior in surface water fluxes by providing additional energy losses by friction in areas where vegetation is present. However, research in this area has been slow for two primary reasons: (1) only within the past few decades has the paradigm in geomorphology shifted from physical processes setting the constraints for biota to a perspective which includes mechanisms by which biota

Figure 1.2: Aerial image of vegetation patches in the Barataria Basin, near the site of an upcoming sediment diversion and marsh creation project. (Image source: [*NOAA*, 2017])

"feeds back on, directly modifies, and contributes to the shape of their physical environment" [*D'Alpaos et al.*, 2016]; and (2) a number of ecogeomorphic feedbacks exist between vegetation, flow, sediment, and nutrients that makes many physical processes difficult to study in isolation [*Corenblit et al.*, 2007; *D'Alpaos et al.*, 2016; *D'Alpaos and Marani*, 2016].

Despite this, some progress has been made in this research area at a range of spatial scales of influence. At the scale of patches (also called canopies or meadows), the flow around complex morphologies of individual stems becomes unimportant, and their effects on hydrodynamics can instead be parameterized using emergent characteristics of the patch [*Nepf*, 2012a; *Luhar and Nepf*, 2013]. Experiments and modeling results show that the spatial structure of vegetation patches can control local hydrodynamics and turbulence production [*Luhar et al.*, 2008; *Nepf*, 2012a,b; *Luhar and Nepf*, 2013; *Meire et al.*, 2014]. Aquatic vegetation

can also affect sediment transport, though whether it enhances deposition (by slowing flow and/or shielding the bed) or enhances resuspension (through the production of turbulence, or scour zones around the patch) depends on the physical structure and density of the macrophytes [*Luhar et al.*, 2008; *Follett and Nepf*, 2012; *Ortiz et al.*, 2013; *Meire et al.*, 2014; *Van Oyen et al.*, 2014]. At the reach scale, vegetation can control the shape of the residence time distributions (RTD) in wetlands, which is an important control parameter for biogeochemical nutrient processing [*Kadlec and Wallace*, 2008; *Cheng and Basu*, 2017; *Hiatt et al.*, 2018].

It is feasible that these hydroecogeomorphic interactions could have notable implications for hydrological connectivity in river deltas. Vegetation in wetlands often self-organizes into patches of varying scales, species, and stem densities [*Addicott et al.*, 1987; *Fonseca and Bell*, 1998; *Oborny et al.*, 2007; *Larsen and Harvey*, 2010; *Vandenbruwaene et al.*, 2011], and in river deltas is generally more populous near the proximal end of deltaic islands and along channel levees [*Carle*, 2013; *Olliver and Edmonds*, 2017] (for examples of deltaic vegetation, see Figures 1.2 and 2.1b). Studies such as *Larsen and Harvey* [2011] and *Larsen et al.* [2017] examined surface-flow through regions of heterogeneous vegetation and developed useful expressions for effective roughness in landscapes of varying anisotropy, patch coverage, and flow depth. However, such studies have yet to extend beyond the vegetated section of the landscape to determine the effects of heterogeneity at the system scale. In deltaic systems, the interaction at the boundary of the vegetated islands and the distributary channels is of primary importance to the hydraulics of the entire delta complex, including the delivery of solids and solutes to the island interior. Thus, it is important to quantify how these local patch-driven effects influence hydrodynamics and connectivity at the system scale.

1.5 Research Questions

The present thesis aims to provide insight into the following research questions:

1. To what extent does the spatial-variability of deltaic vegetation — specifically, percent cover, patch size, and stem density — affect channel-island hydrological connectivity?

2. In addition to flow, what are the implications of vegetation characteristics on the transport dynamics of nutrients and sediment through the system? Can these dynamics inform the ecogeomorphic evolution of deltaic wetlands towards stable vegetated states?

3. What does this mean for our ability to effectively model deltaic restoration efforts? Under what circumstances can models approximate vegetation as uniform?

1.6 Hypotheses

The following hypotheses are tested:

1. *Heterogeneous vegetation will have a different signature on the hydrodynamics of the delta complex than does uniform vegetation.* The more clustered the island roughness, the less we should expect island flow to flow homogeneously. Some distributions of heterogeneous vegetation should be better approximated as uniform than others. Moreover, these effects will not only affect fluid flow, but also the transport of solutes.

2. *An increase in vegetative percent cover and patch roughness will decrease channel-island connectivity.* Each of these characteristics should increase the average vegetative roughness in the islands, which is known to limit connectivity when vegetative roughness is uniform.

3. The clustering of vegetation patches into one larger patch seems qualitatively more heterogeneous than well-distributed smaller patches. Therefore, if heterogeneity affects deltaic hydrodynamics, *an increase in patch size seems likely to exacerbate those effects.*

Chapter 2: Methods

2.1 Overview of the Wax Lake Delta study site

In the midst of several decades of land loss in coastal Louisiana, a few select locations are actively building land. One of those sites is the Wax Lake Delta (WLD, Figure 2.1a), a small and relatively young delta which has been naturally prograding since it first became subaerial during a flood in 1973 [*Wagner et al.*, 2017]. Located at the mouth of the Wax Lake Outlet, the WLD is just East of the Atchafalaya, whose waters have fed the Wax Lake Outlet since its construction in 1941 by the U.S. Army Corps of Engineers. While its original purpose was simply to alleviate flooding of the Atchafalaya in Morgan City, the project has since been regarded as a prime example of a successful sediment diversion [*Kim et al.*, 2009b; *Paola et al.*, 2011]. Both the Atchafalaya River and the Wax Lake Outlet are fed by the Mississippi River, the latter receiving an average of about $110km^3$ of water and 20.5×10^6 metric tons of sediment per year [*Allison et al.*, 2012]. Between 1973 and the present, the WLD has built approximately $35km^2$ of new land [*Allen et al.*, 2012].

Due to the lack of anthropogenic modification, the WLD is now a frequent study site for research aiming to increase our understanding of the physical and biotic processes that drive the natural evolution of deltaic systems [e.g. *Shaw et al.*, 2013, 2016a; *Wagner et al.*, 2017; *Shields et al.*, 2017; *Olliver and Edmonds*, 2017; *Xing et al.*, 2017], including several of the aforementioned studies on structural and functional connectivity [*Hiatt and Passalacqua*, 2015; *Sendrowski and Passalacqua*, 2017]. Vegetation in the WLD tends to be spatially heterogeneous (Figure 2.1b) in terms of species and spatial extent, at least during many seasons of the year. A few specific species of vegetation dominate the ecology of the WLD. The superelevated and rarely-inundated parts of the delta are predominantly populated

Text and figures from this chapter have been submitted in an article to Geophysical Research Letters with Kyle Wright, Matthew Hiatt, and Paola Passalacqua as authors.

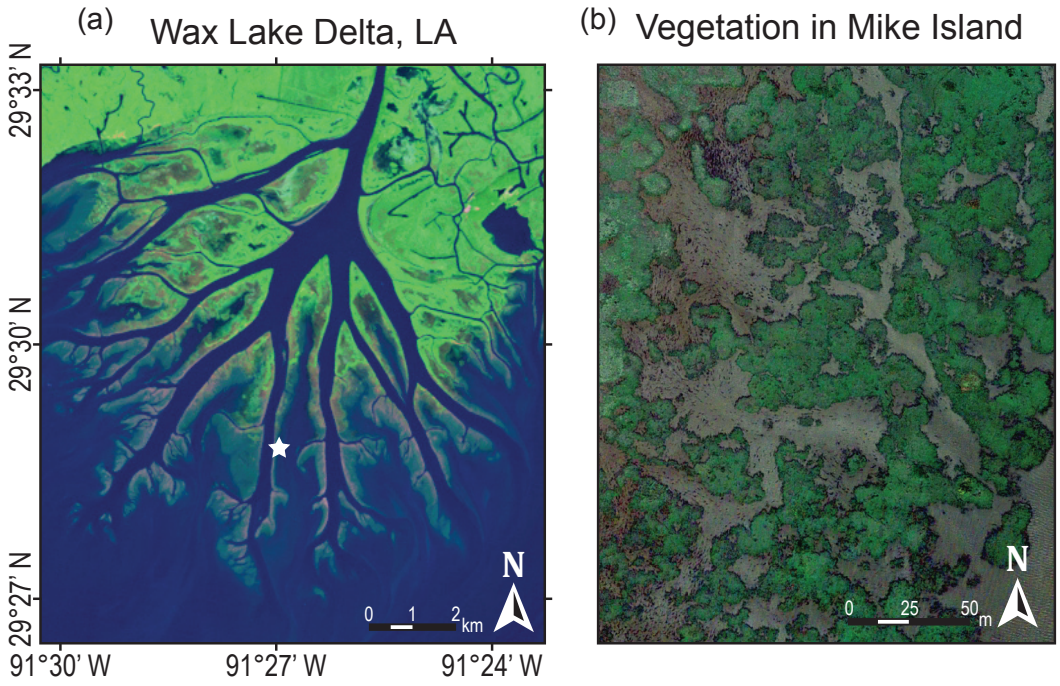

Figure 2.1: The Wax Lake Delta (WLD) in Louisiana, USA. **(a)** False-color LANDSAT imagery of the WLD in October 2011. **(b)** Aerial imagery of deltaic vegetation along the levee of Mike Island (location of white star in (a)) demonstrating spatial complexity.

by *Salix nigra* (black willow), *Colocasia esculenta* (elephant ear), and *Polygonum punctatum* (dotted smartweed) [*Carle*, 2013]. In the lowest-elevated parts of the islands, grasses occupy most of the land, whereas most of the inundated areas are occupied by emergent or floating vegetation, such as *Nulembo lutea* (American lotus) [*Carle*, 2013]. Many of these species are also perennial, which leads to large differences in vegetated extent between the vegetated minimum and maximum most years [*Olliver and Edmonds*, 2017].

Due to the abundant information available on the WLD, it serves as the natural analog for the numerical modeling done in the present study. Our modeling domain is intended to serve as a proxy for the WLD, and the vegetation characteristics, sediment sizes, and flow rates modeled herein were chosen to match those of the WLD complex.

2.2 Numerical model description

2.2.1 Overview of hydrodynamic model (FREHD)

We model hydrodynamics using the Fine Resolution Environmental Hydrodynamics model, or Frehd [*Hodges*, 2014]. This model is used to numerically solve for the steady-state solution of the depth-integrated shallow water equations, using the computational schemes of *Casulli and Cheng* [1992], *Casulli and Cattani* [1994], *Hodges et al.* [2000], *Stelling and Zijlema* [2003], *Hodges* [2004, 2014], and *Hodges and Rueda* [2008]. For further details on the application of Frehd to a deltaic setting, see *Hiatt and Passalacqua* [2017]; *Hiatt et al.* [2018]. The depth-integrated shallow water equations may be written as

$$\frac{\partial \eta}{\partial t} + \frac{\partial}{\partial x} HU + \frac{\partial}{\partial y} HV = 0 \tag{2.1}$$

$$\frac{\partial U}{\partial t} + U\frac{\partial U}{\partial x} + V\frac{\partial U}{\partial y} + g\frac{\partial \eta}{\partial x} - \nu_e \left(\frac{\partial^2 U}{\partial x^2} + \frac{\partial^2 U}{\partial y^2} \right) + \frac{C_R U \sqrt{U^2 + V^2}}{2H} = 0 \tag{2.2}$$

$$\frac{\partial V}{\partial t} + U\frac{\partial V}{\partial x} + V\frac{\partial V}{\partial y} + g\frac{\partial \eta}{\partial y} - \nu_e \left(\frac{\partial^2 V}{\partial x^2} + \frac{\partial^2 V}{\partial y^2} \right) + \frac{C_R V \sqrt{U^2 + V^2}}{2H} = 0 \tag{2.3}$$

in which U and V are the depth-averaged velocities ($m\ s^{-1}$) in the x and y directions respectively, H is the flow depth (m), η is the free surface elevation (m), g is the gravitational acceleration ($m\ s^{-2}$), ν_e is a horizontal eddy-viscosity ($m^2\ s^{-1}$), and C_R is the hydraulic drag coefficient ($-$). We assume viscosity to be negligible, and that local turbulence dissipation is dominated by bed and vegetated drag forces, which is a suitable assumption for subcritical, shallow flow. A constant eddy-viscosity value of $\nu_e = 0.01\ m^2\ s^{-1}$ is assumed for all model runs (*Hiatt et al.* [2018] and the supporting information therein).

2.2.2 The channel-island complex

The domain bathymetry is an idealized channel-island complex (CIC) modeled after the topography and bathymetry along Gadwell Pass at the WLD [*Shaw et al.*, 2016a; *Hiatt and Passalacqua*, 2017]. The CIC (Figure 2.2a) is a 7.5km long by 2km wide domain composed of a 500m-wide central distributary channel and

two adjacent interdistributary islands. The main channel extends 15km through the CIC with an adverse bed slope of 1.33×10^{-4} (the slope of Gadwell Pass).

To ensure that boundary effects are negligible, the CIC is nested within a larger computational buffer domain with a 7.5km wide receiving basin, and a main channel that extends upstream 100km to capture hydraulics over the full backwater zone [*Hiatt and Passalacqua*, 2017]. The upstream slope was constructed to match that of the Atchafalaya River (7×10^{-5}). Previous work has shown that the amount of channel-island connectivity is not strongly influenced by incoming discharge across a range of reasonable values [*Hiatt and Passalacqua*, 2017]; thus, the inflow is set to a constant $700 m^3 s^{-1}$. The model is run on a Cartesian 50m uniform grid, but select model runs are duplicated at 25m resolution, to ensure that discretization effects are negligible (Table A.1).

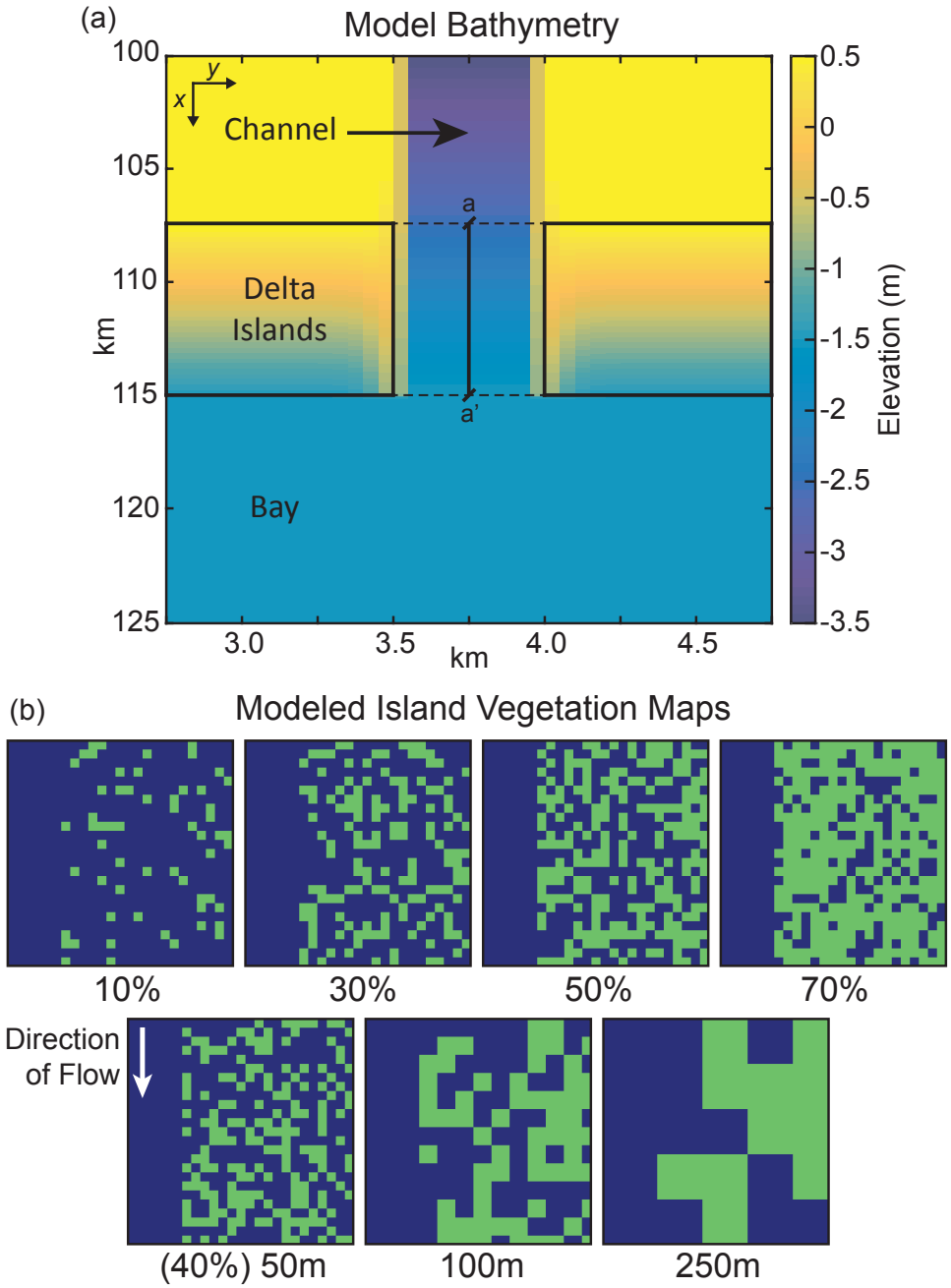

Figure 2.2: Our modeling domain. **(a)** Model bathymetry for the channel-island complex (CIC). Note the horizontal exaggeration. CIC geometry is based on the distributary channels of the Wax Lake Delta (WLD) in Louisiana, USA. **(b)** Sections of spatially-variable (patchy) vegetation maps. In the upper row, percent vegetative cover increases from 10% to 70%. In the lower row, patch size increases (at 40% cover) from 50m to 250m wide square patches.

2.2.3 Vegetation maps: Generation and treatment

Vegetation is modeled in the present study by modifying the hydraulic drag coefficient C_R in Equations (2.2) and (2.3) to account for the additional vegetative flow resistance for all vegetated cells in the domain. The modified bed roughness is calculated using the Baptist equation [*Baptist et al.*, 2007], which may be written as:

$$C_R = \frac{1}{2} C_D n h_v + C_b \tag{2.4}$$

in which C_R is the modified drag coefficient, C_D is the coefficient of drag around a cylinder (*Nepf* [2012a]; assumed to equal unity), n is the vegetation frontal area per unit volume (m^{-1}), h_v is the submerged vegetation height (m), and $C_b = 0.005$ is a typical bed roughness for natural channels [*Nardin et al.*, 2016]. In using this equation as written, we assume vegetation is emergent — however, this equation can be modified to include submerged vegetation, and the values of C_R used herein could just as well represent a mix of emergent and submerged vegetation.

All models were run at two stem density values, i.e. selected values of the product nh_v: the first ($nh_v = 0.1$) near the transition from sparse to dense vegetation, and the second ($nh_v = 3.0$) in the upper range of dense vegetation [*Luhar et al.*, 2008; *Li et al.*, 2015]. We henceforth refer to these simply as "sparse" and "dense" scenarios, respectively. Here, the words "sparse" and "dense" are only a naming convention, meant in a relative sense, and are not meant to carry with them the physical implications of these terms from the study of submerged vegetation. A dense patch of vegetation is one which imparts more resistance onto the flow than a sparse patch. Selected scenarios have also been run at two intermediate values, ($nh_v = 0.5, 1.0$). For all non-vegetated cells in the domain, $C_R = C_b$.

Several scenarios were considered for the study of spatially-variable vegetation, including:

1. Maps in which island vegetation decreases uniformly in the direction of the bay according to some defined function (e.g. linear, logarithmic)

2. Maps in which the islands are populated by randomly distributed patches of a defined size and percentage of island covered (also called "uniform random

maps")

3. Maps in which the islands are populated by randomly distributed patches, but with patch characteristics (density, percent cover) that vary spatially throughout the island, such that the resulting distribution looks like deltaic vegetation (e.g. more vegetation upstream and along levees; also called "gradient random maps," or GRM)

While each of these options have their merits, in our present analysis we choose to focus on uniform random maps, which are considered a neutral model in landscape ecology [*Gustafson and Parker*, 1992; *Oborny et al.*, 2007]. We expect that they more accurately represent heterogeneity in wetland vegetation than option (1), while also requiring minimal assumptions about the spatial structure of vegetation, on which the results of (3) would likely depend. It is true that (3) would provide the most realistic parameterization of vegetation in any individual system, but the results would potentially lose generality to systems whose vegetation characteristics differ. However, while most of the results and discussion will focus on uniform random maps, examples of each of these alternatives are also modeled and are discussed minimally in section 3.3.

For each random map, vegetation patches are distributed randomly throughout the deltaic islands according to a specified percent cover, patch size, and density (C_R). The modeled random maps (e.g. Figure 2.2b) span a range of coverage values $\in \{10\%, 20\%, 30\%, 40\%, 50\%, 70\%\}$, and patch sizes, which are squares of side length $\in \{50\text{m}, 100\text{m}, 250\text{m}\}$. Note that vegetation "density" refers to the selection of (C_R), and not to the percentage of the island occupied by vegetation. These values were chosen to cover a range of vegetative characteristics one might expect to see in systems like the WLD (Figures 2.1b, 1.2; [*Olliver and Edmonds*, 2017]). For each unique pairing of patch coverage, size, and density, a minimum of five maps are modeled, such that the results can draw upon the behavior of the ensemble rather than any individual initialization of the model. The code for generating these maps is given in Appendix D.

If vegetation patchiness is unimportant, one might expect that the same system behavior would be observed if a single roughness value were applied uniformly within the deltaic islands — such as, for example, the spatially-averaged vegetative

roughness in each island. Effective uniformity would allow for a relatively simple parameterization of vegetation in deltaic models, as was done in prior studies [*Nardin et al.*, 2016; *Hiatt and Passalacqua*, 2017]. Thus, a range of spatially-uniform model runs has also been performed for comparison. These spatially-variable and spatially-uniform runs will henceforth be referred to as "patchy" and "uniform" runs, respectively. For each uniform run, the island roughness corresponds to the spatially-averaged roughness in some patchy run. There exists a corresponding uniform run for each unique pairing of percent cover and patch density in the patchy runs. We expect that the differences in results between each pair of runs represents the role of heterogeneity in the system.

2.2.4 Tracer studies & residence time distributions

For each model run, a pulse of tracer is released in the central channel upstream of the domain of interest at steady state, and the flux of tracer exiting the delta complex at the distal end of the system is monitored through time. The transport of a passive tracer in Frehd is modeled with a conservative advection-diffusion scheme [*Hodges*, 2014] according to the following equation:

$$\frac{\partial cH}{\partial t} + \frac{\partial}{\partial x}UcH + \frac{\partial}{\partial y}VcH - \kappa_e \frac{\partial}{\partial x}\left(H\frac{\partial c}{\partial x}\right) - \kappa_e \frac{\partial}{\partial y}\left(H\frac{\partial c}{\partial y}\right) = 0 \tag{2.5}$$

in which c is the depth-averaged concentration of tracer ($kg\ m^{-3}$) and k_e is the scalar eddy diffusivity ($m^2\ s^{-1}$), which we have assumed to be equal to the momentum eddy diffusivity $\nu_e = 0.01$. The exit age distribution $E(t)$ (also called the residence time distribution, or RTD) can be evaluated as the rate at which tracer exits the domain [*Benjamin and Lawler*, 2013], normalized by the initial mass of the pulse; that is,

$$E(t) = \sum_{x_{B,0}}^{x_{B,N}} \frac{Q_\perp(x_B, t)}{M_{in}} c(x_B, t) \tag{2.6}$$

where $Q_\perp(x_B, t)$ is the local volumetric flow rate ($m^3\ s^{-1}$), M_{in} is the initial mass of the tracer pulse (kg), and $c(x_B, t)$ is the local concentration of tracer, summed over all cells x_B along the boundary. The volumetric flow rate, $Q_\perp(x_B, t)$ is equal to the product $U_\perp(x_B, t) \cdot H(x_B, t)$, where U is the velocity vector normal to the

boundary ($m\ s^{-1}$), and H is the flow depth (m). Because M_{in} is equal to the total amount of tracer that will eventually exit the domain, equation 2.6 can be equivalently written:

$$E(t) = \frac{\sum_{x_{B,0}}^{x_{B,N}} Q_{\perp}(x_B, t) \cdot c(x_B, t)}{\sum_{t=0}^{\infty} \sum_{x_{B,0}}^{x_{B,N}} Q_{\perp}(x_B, t) \cdot c(x_B, t)} \tag{2.7}$$

For each model scenario, these $E(t)$ curves can be separated into the relative contribution of the channel and the islands to the bulk $E(t)$. More formally,

$$E_{total}(t) = E_{isl}(t) + E_{chan}(t) \tag{2.8}$$

The discrete integration of $E(t)$ through time yields $F(t)$, the cumulative fraction of tracer that has exited the domain by time t:

$$F(t) = \sum_{\tau=0}^{t} E(\tau) \tag{2.9}$$

which in the limit as t goes to ∞ converges to unity. The time integration of the channel and island contributions to $E(t)$ can be said to represent the relative fraction of tracer that is allocated to each. As with $E(t)$, $F(t)$ can be equivalently decomposed into $F_{isl}(t)$ and $F_{chan}(t)$. The time-integration of $E_{isl}(t)$ gives the total fraction of tracer allocated to the islands ($F_{isl}(t)$). Studying the transport of the tracer through the CIC allows us to characterize flow patterns and can serve as a proxy for the transport of suspended sediment or nutrients through the system [*Hodges*, 2014].

2.2.5 Calculation of shear velocities

To gain insight into sediment dynamics, flow velocity and depth values are used to calculate shear velocities using the Wilcock equation [*Wilcock*, 1996]:

$$u_* = \kappa \sqrt{U^2 + V^2} \left[ln \left(\frac{H}{e \cdot z_0} \right) \right]^{-1} \tag{2.10}$$

in which u_* is the shear velocity ($m\ s^{-1}$), $\kappa \approx 0.4$ is the von Kármán "constant", and z_0 is the reference roughness height (m). We can approximate the roughness height as $z_0 \approx 0.095 D_{90}$, in which D_{90} is the 90th percentile grain size. In the Wax Lake Delta (WLD), studies have shown that the majority of the deposited sediment is fine sands, with a representative D_{90} of approximately $350 \mu m$ [*Shaw et al.*, 2013].

By comparing shear velocity values to the critical threshold values for motion ($u^*_{crit} = 9.2\ mm/s$) and suspension ($u^*_{sus} = 21.0\ mm/s$) for the $D_{50}\,(210 \mu m)$ in the WLD [*Shaw and Mohrig*, 2014], we can determine where the median grain size is likely to be in incipient motion or suspension within the delta complex.

Chapter 3: Results

3.1 Hydraulic implications of vegetation percent cover, patch size, and stem density at local and system scales

3.1.1 The transition to unconfined flow

Due to hydrological connectivity, we expect to see a marked decrease in the amount of flow that remains confined in the channel moving downstream towards the bay [*Hiatt and Passalacqua*, 2017]. In our model runs, discharge transects in the central channel from the upstream end of the CIC to the bay show between 20%-70% of the channel flow is allocated to the islands (Figure 3.1) for both patchy and uniform vegetation distributions. The fraction of discharge that remains in the channel increases for an increase in average vegetation roughness — which, for the patchy runs, entails either an increase in vegetation coverage or density. Little variation has been observed between runs with the same coverage characteristics, particularly when patches are small.

Patchy and uniform runs differ in connectivity by only a small amount in many of the modeling scenarios — when vegetation patches are sparse, small, and coverage is high, the fraction of discharge allocated to the islands in patchy and uniform runs is closely comparable (e.g. Figure 3.1a). However, when vegetation is dense (more resistant to flow) and covers less than half the domain, the disparity between patchy and uniform runs grows considerably (Figure 3.1b). At 10% cover, roughly 22%-27% more of the channel flow is allocated to the islands in the patchy runs before discharging into the bay. At 40% cover, this disparity shrinks to a smaller but still significant 7%-19%. However, at 70% cover, the behavior between patchy and uniform runs is nearly indistinguishable (1%-3% difference for 50m-100m patches, 7% for 250m). Generally, the disparity is larger for all runs with

Text and figures from this chapter have been submitted in an article to Geophysical Research Letters with Kyle Wright, Matthew Hiatt, and Paola Passalacqua as authors.

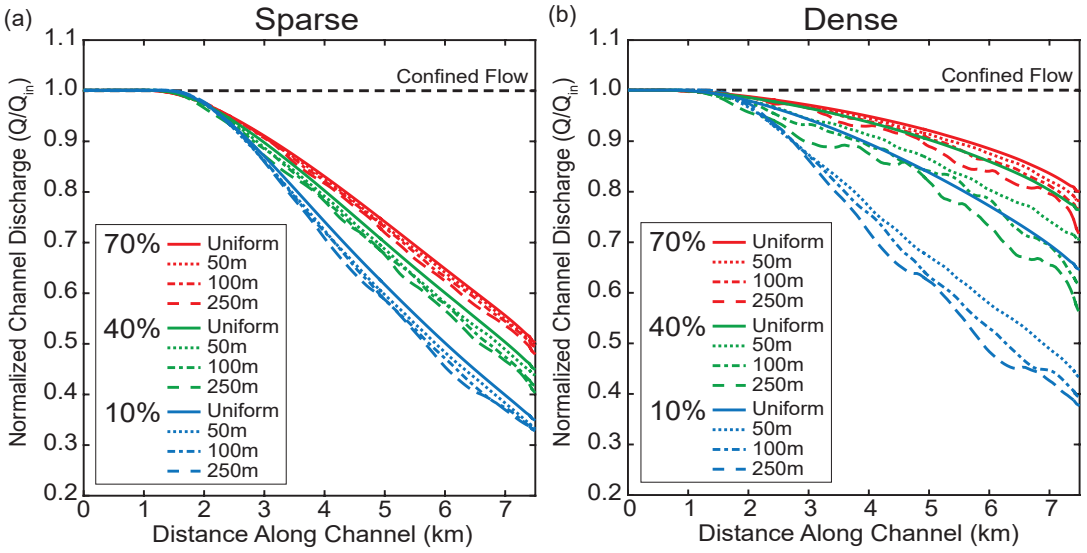

Figure 3.1: Profiles showing the fraction of discharge that remains confined in the channel averaged over the ensemble of select scenarios for **(a)** sparse and **(b)** dense vegetation. The abscissa is collinear with line a-a' shown in Figure 2.2a. These transects correspond to patchy model runs with 10%, 40%, and 70% cover (at all patch sizes), as well as their corresponding uniform-roughness runs. The y-axis is normalized by the discharge of the inflow.

40% vegetation or less, and negligible at 50% or higher (transects for all scenarios are shown in Figure C.3). Each patchy run displaying higher connectivity has a water surface elevation in the channel centimeters to decimeters lower than its corresponding uniform run (Figure 3.2), driven by changes in lateral outflow. As such, certain patchy runs demonstrate considerably different hydrodynamics over the full backwater length.

The amount of flow allocated to the islands also tends to increase with increasing patch size. For runs with larger patches (100m and 250m width), discharge transects typically fall 6%-13% below those for the smallest patches at all coverage values (Figure 3.1), indicating an increase in lateral outflow. The difference between the curves for the smallest and largest patches is of the same magnitude at all coverage values, suggesting that scaling effects are relatively consistent irrespective of other coverage characteristics. Notably, the model runs with larger patches contain the largest deviations from the mean behavior, with flow

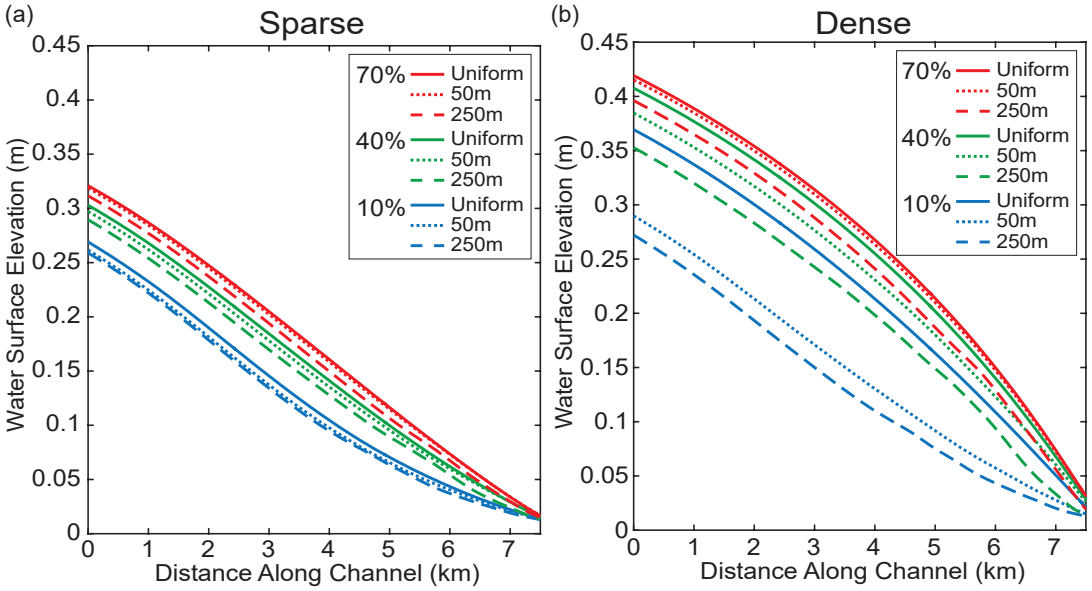

Figure 3.2: Profiles showing the water surface elevations in the main channel for select model scenarios with **(a)** sparse and **(b)** dense vegetation. The abscissa is collinear with line a-a' shown in Figure 2.2a. These transects correspond to patchy model runs with 10%, 40%, and 70% cover (at 50m and 250m patch sizes), as well as their corresponding uniform-roughness runs.

sometimes even being rerouted back into the main channel from the islands. So, while the general trend may indicate an increase in lateral outflow for an increase in patch size, it may not be true for every individual run or at any given transect of an individual run.

3.1.2 Effects on island flow

Having a heterogeneous vegetation distribution creates a heterogeneous flow field in the islands. Maps of velocity magnitude throughout the islands show high spatial complexity for both dense (Figure 3.3a-d) and sparse (e-h) vegetation. Vegetation patches reduce flow velocities within and near patches, but they also elevate velocities in many non-vegetated cells with respect to what is seen in uniform runs. This is particularly true at low coverage values, where high-velocity preferential flow-paths are clearly visible (e.g. Figure 3.3e,f). These flow corridors develop less

frequently as coverage increases (Figure 3.3d). In contrast, all uniform roughness runs display a fairly uniform flow-field within the islands.

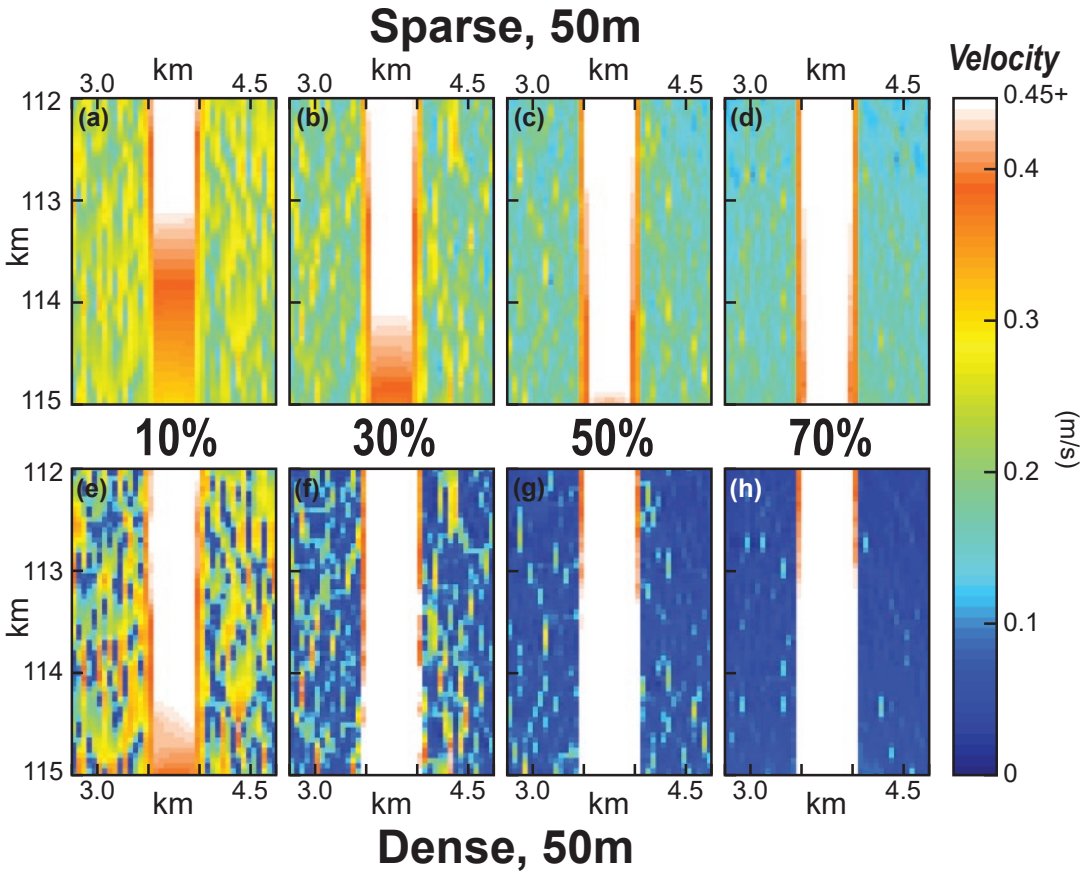

Figure 3.3: Flow and shear velocity magnitudes throughout a representative section of the CIC for sparse **(a-d)** and dense **(e-h)** vegetation. The color axis is truncated to provide the most resolution within the islands. The patches of vegetation not only reduce in-patch flow velocities, but elevate the velocities in non-vegetated cells. At $\leq 40\%$ cover, high-velocity preferential flow-paths develop, particularly when vegetation is dense.

The difference in flow velocities between vegetated and non-vegetated cells also increases as a function of patch density and size, and decreases for increasing coverage. The average velocity in vegetated and non-vegetated cells, as well as the ratio of the two, shows a clear trend for changes in density, coverage, and patch size (Figure 3.4). The mean velocity within vegetated cells is much lower

when density is high, and is similar in magnitude across all patch sizes — though there is a slight decrease for an increase in patch size. The mean velocity in non-vegetated cells shows a clear decreasing trend for increases in percent cover, and differences are more pronounced between runs of different patch size. The ratio of vegetated and non-vegetated velocities (Figure 3.4c-d) shows a near-linear increase for increases in percent cover, indicating that vegetated and non-vegetated cells have increasingly similar mean velocities at high percent cover. Larger patch sizes lead to larger differences and thus lower ratios at all coverage values.

To ensure that each ensemble of patchy runs with identical vegetation characteristics were statistically similar, the distribution of flow velocities throughout the vegetated islands is compared using Wilcoxon rank-sum tests. For each unique pairing of coverage, patch size, and density, each of the five runs from different random initializations are compared to each of the others (i.e. a total 10 comparisons) and the p values are tabulated. Most runs representing the same characteristics are statistically similar – with the threshold for "similarity" set by the typical p value of comparing runs with different vegetation characteristics. Runs with larger patch sizes tend to be more dissimilar than those with smaller patch sizes, but still typically fall below the threshold. See Appendix B for details.

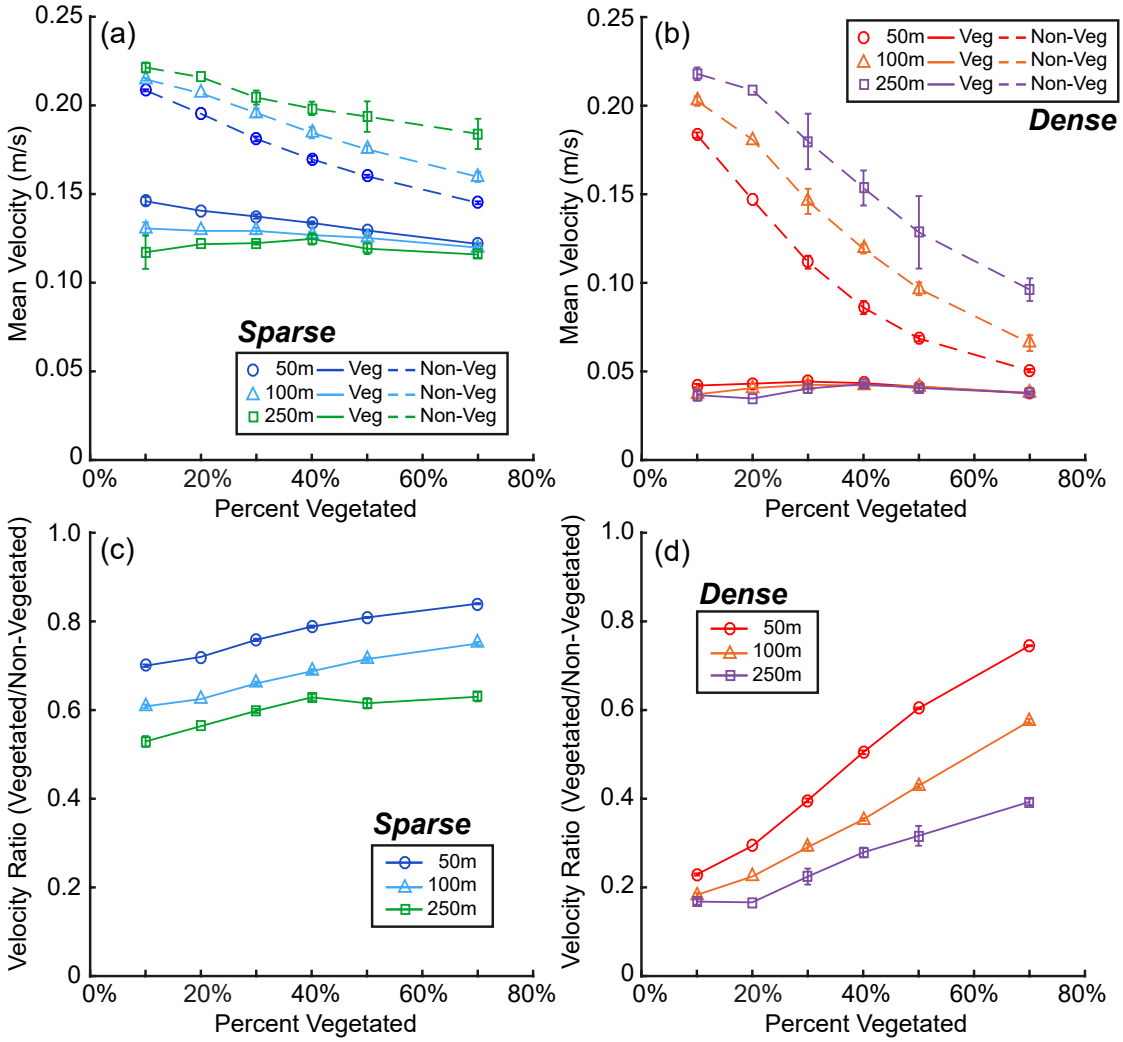

Figure 3.4: Comparison of mean velocities in vegetated and non-vegetated island cells. **(a-b)** The mean velocity in the vegetated (solid lines) and non-vegetated (dashed lines) island cells for all model runs at each patch size for sparse (a) and dense (b) vegetation. The error bars represent the standard deviation of the means of the ensemble. **(c-d)** The ratio of the vegetated and non-vegetated velocities shown in (a-b) for sparse (c) and dense (d) vegetation. The ratio approaches unity at high percent cover values, indicating that vegetated and non-vegetated cells have increasingly similar average velocities.

3.2 Patchiness and transport: the enhanced delivery of solutes to the island interior

3.2.1 Allocation of the tracer in the channel-island complex

Releasing a passive tracer upstream of each model scenario allows for the construction of fractional mass-flux curves ($E(t)$) at the bay end of the domain. These curves represent the residence time distributions (RTD) for each scenario, which can be decomposed into the marginal contribution of the channel ($E_{chan}(t)$) and islands ($E_{isl}(t)$) to the bulk RTD (e.g. Figures 3.5a-b, 3.6a-b, C.1). Generally, each RTD contains a tall peak corresponding to the main channel, through which some of the tracer exits the domain all at once — followed by a shorter, longer-lived tail corresponding to the islands that decays exponentially. The relative contributions of the channel and islands to the RTD depend on the amount of flow allocated to each. The RTD for all uniform runs is relatively smooth with a single peak, whereas the RTD for patchy runs is often multi-modal, with a more rapid decay. Each patchy run has an RTD that is visually similar to its respective uniform run, but different runs with the same coverage characteristics are more variable due to the random placement of vegetation (for examples, see Figure C.1). At what time the variations occur depends upon each individual roughness map. The relative sizes of local maxima tend to increase with patch size.

Integrating each of the mass-flux curves through time yields the cumulative flux of tracer ($F(t)$) through the CIC, which goes to unity as $t \to \infty$. Likewise, the time-integration of $E_{isl}(t)$ gives the total fraction of tracer allocated to the islands ($F_{isl}(t)$). For the range of scenarios tested herein, the total fraction of tracer allocated to the islands ranges from 0.2 to 0.7 (e.g. Figures 3.5c-g and 3.6c-g). For model runs with uniform vegetation, this value varies linearly as a function of the logarithm of the island roughness (for details see Figure C.2). All $F_{isl}(t)$ curves for uniform vegetation fall below those of patchy vegetation. At 40% vegetation or less, large differences are clearly visible between $F_{isl}(t)$ curves for uniform and patchy runs, particularly for dense vegetation. Some patchy runs (e.g. Figure 3.5d) show over twice the amount of tracer allocated to the islands as the uniform scenario would predict. At 50% vegetation or greater, however, the disparity shrinks such that most curves differ by only a few percent (Figure

3.5e-f). For small patch sizes, the disparity decreases gradually, whereas for the larger patch sizes, there exists more of a step-like threshold near 50% at which the tracer flux decreases considerably. For sparse vegetation, $F_{isl}(t)$ curves follow a similar trend, but to a lesser extent (Figure 3.6).

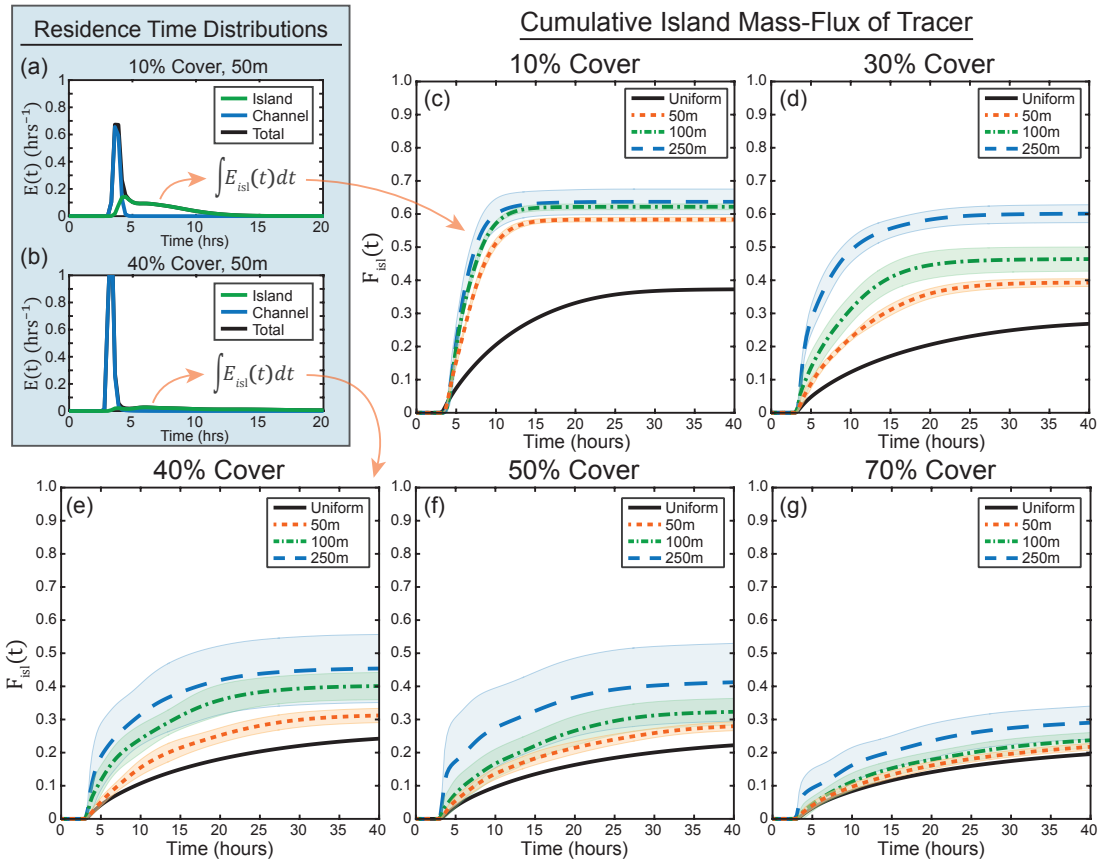

Figure 3.5: Fraction of the tracer allocated to the islands through time. **(a-b)** Example RTD calculated using mass-flux breakthrough curves at the bay end of the CIC, decomposed into channel and island contributions. **(c-g)** Time-integrated form of $E_{isl}(t)$, the island contribution to the RTD. Higher values imply larger tracer flux into the islands. Each plot shows $F_{isl}(t)$ curves for patchy runs at all patch sizes (and the corresponding uniform run) for a given percent cover. Shaded regions delineate ± 1 standard deviation. Patchy and uniform runs differ considerably at low coverage values (c-e). There appears to be a threshold near 50% cover (e-f), above which patchy and uniform runs converge to very similar temporal behavior (f-g).

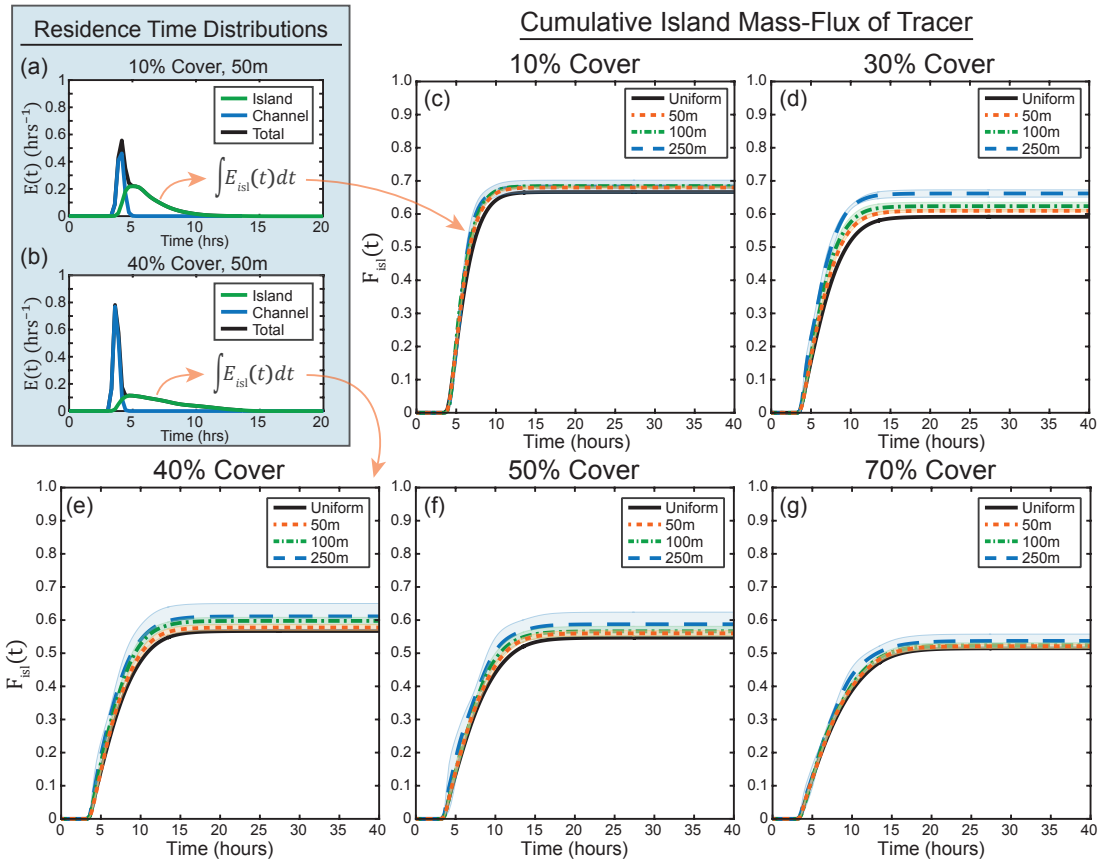

Figure 3.6: The same as Figure 3.5 but for sparse vegetation. As with dense vegetation, the largest differences between patchy and uniform runs appears to occur below a threshold near 50% cover (e-f), above which patchy and uniform runs converge to approximately the same temporal behavior (f-g). However, these differences are less pronounced for sparse vegetation.

3.2.2 Diminishing tracer flux for an increasing stem density

Several patchy model runs were also repeated for intermediate values of the patch density, with values of $nh_v = 0.5, 1.0$. Because patchy and uniform runs differed most at around 30% vegetated cover, these models were run for all patch sizes at 30%. The intention of these runs is to be exploratory — to determine how the system behaved in the transition from sparse to dense vegetation — which is why these runs were not repeated on the exhaustive list of percent cover values.

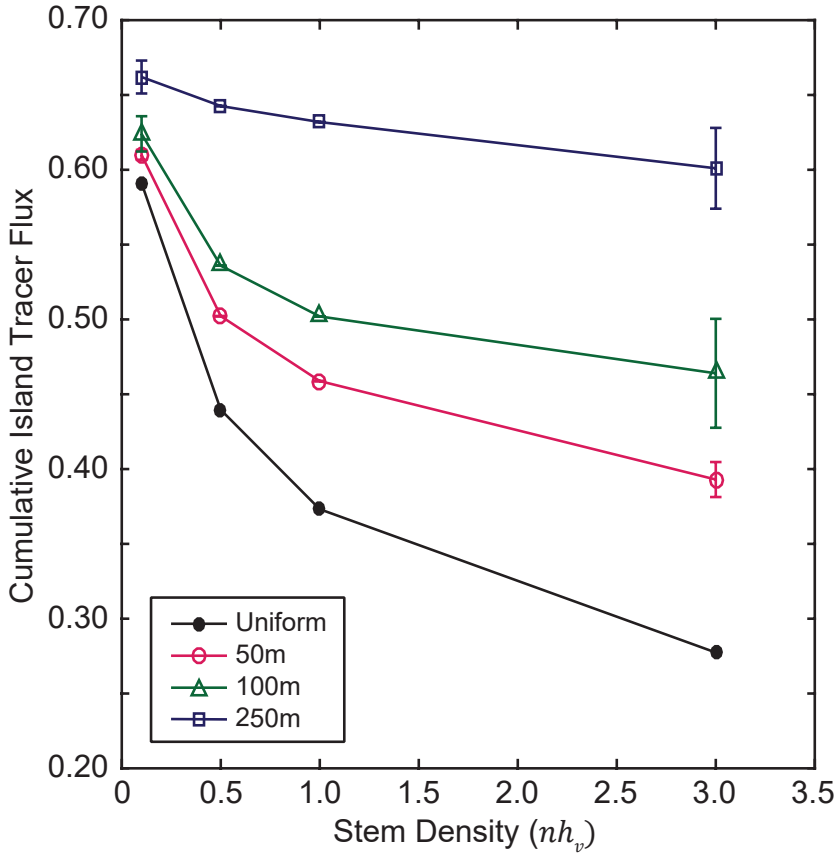

Figure 3.7: The cumulative amount of tracer allocated to the islands vs vegetation stem density at 30% cover. For uniform runs, the decrease in island flux is a function of the logarithm of the stem density. For patchy runs, the trend is similar, but the decay is slower. At large patch sizes, plant density does not seem to significantly affect island tracer flux.

Perhaps the most illustrative trend for an increase in density occurs in the proportion of tracer allocated to the islands. For fully uniform runs, the total cumulative flux of tracer into the islands decreases for an increase in island roughness. This trend is almost perfectly log-linear, i.e. the tracer flux decreases linearly proportional to the logarithm of the roughness (this trend can be seen in full in Figure C.2, but the relevant portion is also shown as the black line in Figure 3.7). For patchy runs, this log-linear behavior nearly holds for small patches (magenta line in Figure 3.7) and becomes increasingly linear-linear for larger patches (blue

line). All patchy runs show a noticeable increase in the island tracer flux when compared to the uniform runs. Additionally, the difference between the uniform and patchy runs increases for an increase in density, as we should expect from the previous results. This finding retroactively provides insight into what could reasonably be considered "sparse" and "dense" scenarios: "sparse" vegetation has an nh_v value small enough ($\leq \mathcal{O}(0.1)$) that inhomogeneity is negligible, whereas "dense" vegetation has an nh_v large enough ($\geq \mathcal{O}(1)$) for these differences to be considerable.

3.2.3 Fate and transport of sediment

As a fairly straightforward extension of the velocity maps shown in section 3.1.2, maps of shear velocities reveal a similarly complex picture (Figure 3.8). For all uniform runs, we observe nearly identical behavior: shear velocities $< u^*_{crit}$ everywhere in the islands, and $> u^*_{sus}$ everywhere in the main channel, with some cells in the range of incipient suspension along the subaqueous levees. For patchy runs, however, shear velocities in large sections of the islands are elevated above u^*_{crit} into incipient suspension, primarily along channelized flow-paths. As vegetative cover increases, shear velocities converge to match the spatial trend of the uniform runs.

We find that a significant portion (though not all) of the cells within vegetation patches remain $< u^*_{crit}$ at all coverage values, while only a small percentage of the non-vegetated cells remain within the range of no motion. For example, at 10% (dense) vegetation cover, 70%-80% of the non-vegetated cells in the islands have shear velocities above the threshold of motion. This number decreases with increasing coverage, and becomes nearly zero at around 50% vegetation cover.

3.3 Other roughness maps

Aside from the uniform maps, the results from modeling several other spatially-variable scenarios (Figure 3.9) are briefly mentioned. The first two are maps with uniformly decreasing roughness toward the distal end of the channel-island complex (Figure 3.9a-b). The latter two are gradient random maps (GRMs), in which the linearly decreasing island roughness is superimposed on a mosaic of

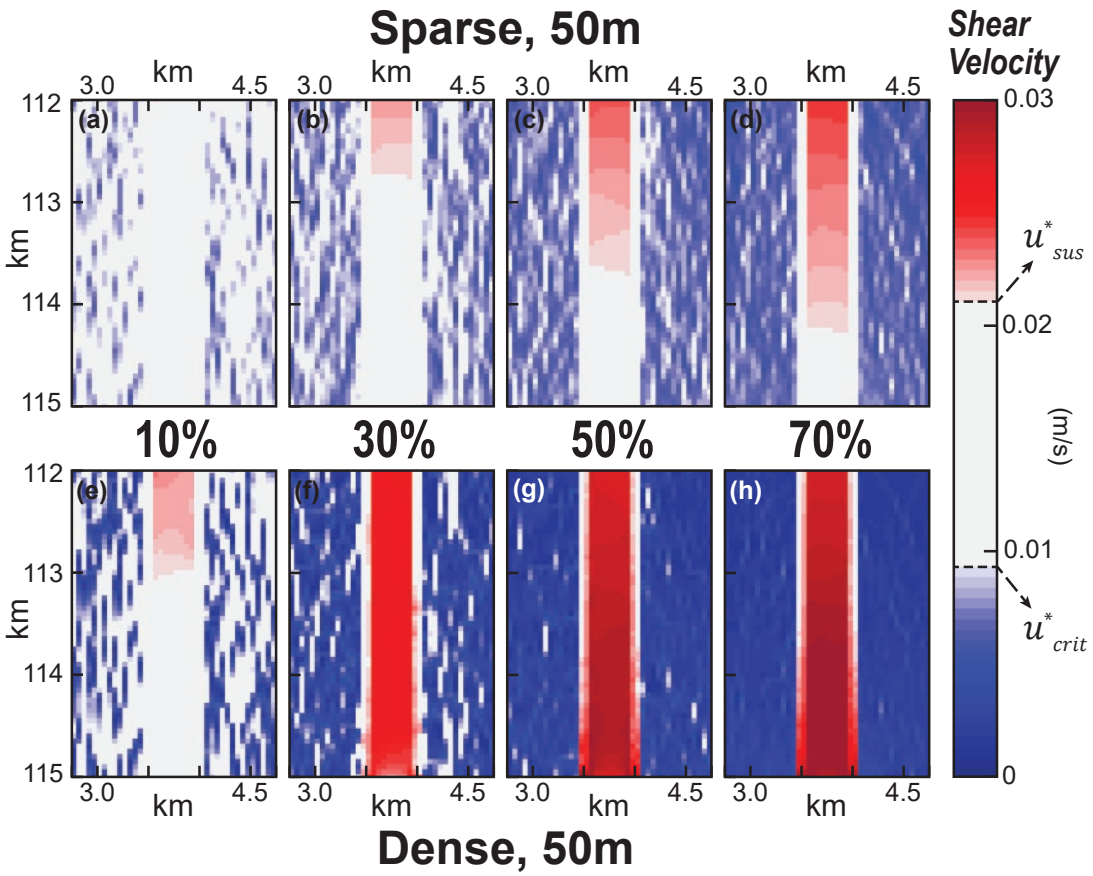

Figure 3.8: Calculated shear velocity (u^*) values for the same section of the domain as those shown in Figure 3.3 for sparse **(a-d)** and dense **(e-h)** vegetation. In contrast to uniform-roughness runs, for which island shear velocities are all $\leq u^*_{crit}$, greater transport potential exists when vegetation is heterogeneous.

random patches, which decrease in percent cover in the island interiors as well as in the more distal end of the system (Figure 3.9c-d).

The GRM maps provide some first-order exploration of the effect of vegetation seasonality. This is done by varying the percent cover in the island interior while maintaining approximately the same amount of vegetation in the proximal end of the delta, as well as along the channel levees. These example maps are dubbed "summer" and "winter" scenarios, respectively 3.9c-d), though they do not intend to accurately represent conditions in natural systems for which actual

coverage characteristics are unknown.

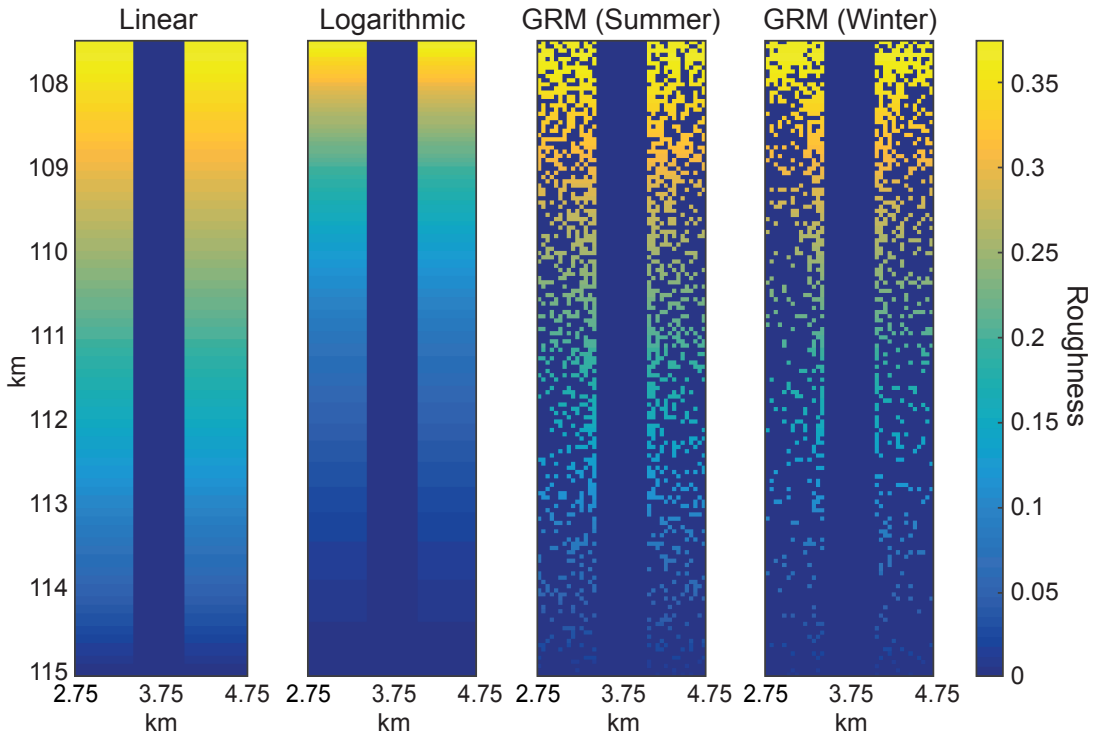

Figure 3.9: Other spatially-variable roughness maps that have been modeled. **(a)** Linearly decreasing island roughness. **(b)** Logarithmically decreasing island roughness. **(c-d)** Example gradient random maps (GRM) where roughness and percent cover decrease in the interior of the island and in the downstream direction. (d) has a lower percent cover along the island interior, where seasonal vegetation is more populous. The comparison between (c) and (d) is intended to explore the difference in connectivity between a feasible vegetation maximum and minimum.

For model runs with linearly/logarithmically decreasing island roughness, we observe similar behavior to systems with uniform island roughness, with the primary difference being the location at which lateral outflow begins to occur. The onset is generally delayed with respect to uniform runs and increases in magnitude moving downstream. Aside from this change in shape of the outflow curve, spatial-variable vegetation of this type does not seem to have any other significant effects on the hydraulics of the system.

For the GRM maps tested, we find (somewhat unsurprisingly) that the

behavior lies in between that of the decreasing island roughness and that of the patchy uniform random maps. The curve representing the transition to unconfined flow has a shape similar to that for the uniformly decreasing island roughness scenarios, with a slight increase in connectivity with respect to those scenarios due to the formation of connected flow-paths in the islands. The fact that GRM runs still demonstrate an increase in connectivity when high-velocity flow-paths form in the island interior demonstrates that these flow-paths do not have to connect to the central distributary channel for there to be a visible increase in connectivity. Therefore, it stands to reason that the prior results shown for uniform random maps would still hold true even when there exists a higher proportion of vegetation along the island levees, as is typically the case in natural systems.

It is, however, difficult to determine which of the observed hydraulic effects are due to the decreasing density, the decreasing coverage downstream, or the decreasing coverage towards the inside of the island. The results from these maps are included only to emphasize that the observed threshold behavior appears to persist even when the presence of vegetation is more pronounced on the levees.

Chapter 4: Discussion

4.1 Disconnectivity above a vegetation cover threshold

4.1.1 Connection to percolation theory

The hydraulic and tracer results (Figures 3.1 and 3.5) reveal a noticeable change in hydrological connectivity near 40%-50% vegetation cover, particularly for dense vegetation. This seems to suggest that some form of threshold exists in connectivity near that value. Above the threshold, patchy and uniform scenarios differ minimally at the system scale — the island flow is approximately homogeneous, and the same amount of lateral outflow is observed regardless of patch characteristics. Below the threshold, however, uniform runs consistently underestimate the degree of connectivity observed in patchy runs. For sparse vegetation, the effects of this threshold are visible, but small. Only when patches are dense do the effects become substantial.

We attribute this to the fact that high-velocity preferential flow-paths are able to develop within the islands at low coverage values (Figure 3.3a-b,e-f), which are able to draw a higher proportion of the flow from the main channel. These flow corridors increase the transport capabilities through the islands, as quantified by the RTD and $F_{isl}(t)$ curves. Below this "disconnectivity" threshold, uniform model runs with an equivalent spatially-averaged roughness poorly capture the behavior of model runs in which heterogeneity is modeled explicitly. Uniform model runs with other estimates of mean roughness, such as the geometric or harmonic mean, were not any more capable of capturing these dynamics, nor were models using other uniform estimates for effective resistance, such as blockage factor [*Nepf*, 2012a] (results not shown).

The observed threshold behavior appears to match that predicted by isotropic

Text and figures from this chapter have been submitted in an article to Geophysical Research Letters with Kyle Wright, Matthew Hiatt, and Paola Passalacqua as authors.

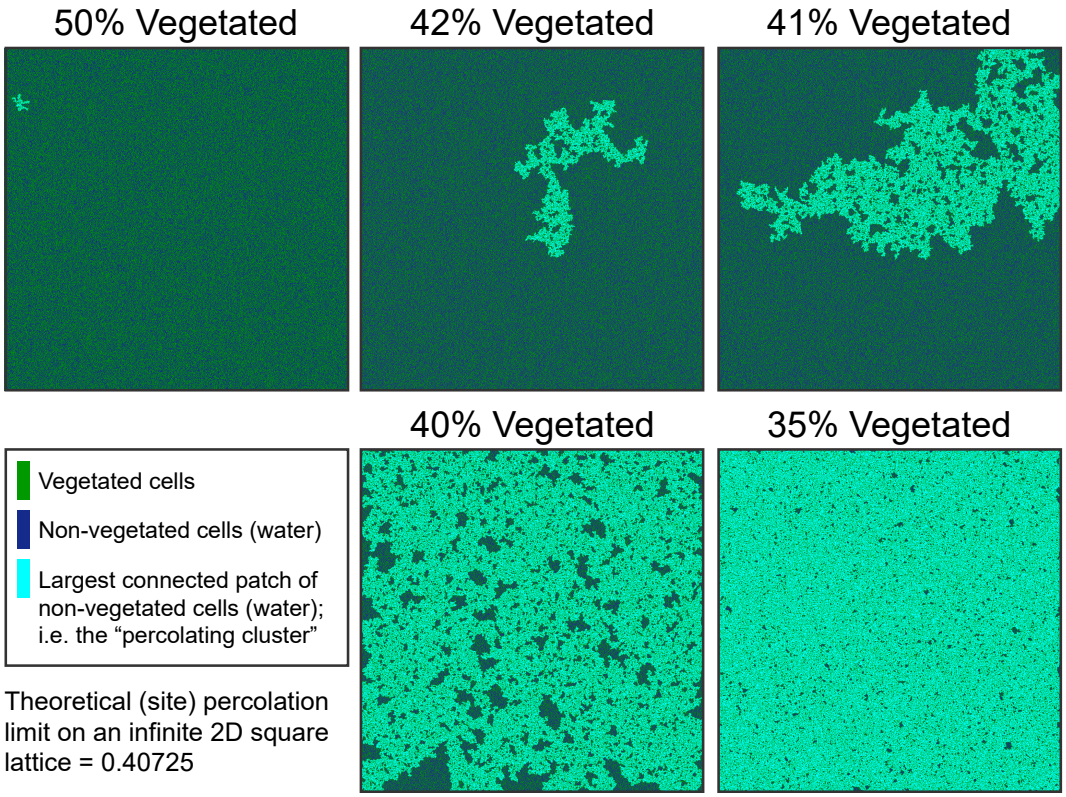

Figure 4.1: Demonstration of the percolation limit on a 1000 x 1000 square lattice. For each lattice, the percent vegetated is equal to the probability of each cell in the lattice being "occupied" by vegetation. The largest contiguous cluster of non-vegetated cells is highlighted in light blue. As percent cover decreases from 50% to 35%, the "percolating cluster" spans the full domain near the theoretical percolation threshold of $\approx 41\%$.

percolation theory. This theory describes a threshold change in the connectivity of "occupied" cells in a binary domain — which, in our case, would represent vegetated cells vs non-vegetated cells — once a specific percentage of the domain is occupied. Used in this sense, the word "connectivity" describes the contiguity of a cell with other cells in the same von Neumann neighborhood [*Oborny et al.*, 2007]. On a 2D square lattice, a critical transition is predicted to occur once more than about $\geq 59\%$ of the cells are occupied [*Stauffer*, 1979]. This transition is only approximate for finite domains, and becomes increasingly step-like as the size of

the domain approaches infinity.

If our system is analogous, one might expect islands to channelize once $\geq$ 59% of the domain is non-vegetated — or, equivalently, once $\leq$ 41% of the domain is vegetated. This is indeed what we observe in our model runs. The mathematical details of percolation theory are complex and not particularly important for the present discussion (for good overviews on percolation theory, see *Stauffer* [1979]; *Hunt and Sahimi* [2017]), but qualitatively, the theory provides insight and a potential explanation for the threshold we observe in our system. Figure 4.1 demonstrates what the percolation transition looks like on a much larger domain (1000×1000 cells) than that of our deltaic islands; there is a critical shift in connectivity at the percolation threshold, from a state where every non-vegetated cell in the domain is relatively isolated to a state where nearly all of them are connected.

Some studies hypothesized that a percolation-style threshold could exist in ecological systems [*Oborny et al.*, 2007; *Luhar et al.*, 2008; *Larsen et al.*, 2017], with vegetation patches possibly self-organizing near this threshold to maximize nutrient delivery [*Fonseca and Bell*, 1998; *Luhar et al.*, 2008]. We believe the results of the present study lend credibility to those hypotheses. Our study also indicates that the effects of preferential flow-paths extend beyond the vegetated domain, by providing a control on hydrological connectivity with the main channel. It is also interesting that we observe this threshold despite the fact that, from the perspective of flow, our islands are not strictly binary (flow is still permitted through vegetated cells).

One notable caveat, however, bears consideration: there is not only one percolation threshold. The actual value at which the transition occurs depends on the shape of the cells comprising the lattice. For 2D fields, the critical transition could occur at 41% (for a square lattice), but it could also occur anywhere from 30% (honeycomb) to 50% (triangular) [*Hunt and Sahimi*, 2017]. Therefore, because vegetation in real systems would not strictly adhere to any of these shapes, we should not expect that the disconnectivity threshold in natural systems be exactly 41%. Rather, these results simply indicate that such a threshold can exist, and wherever it may lie in any given system, it can substantially influence hydrological connectivity and flows through the vegetated domain.

4.1.2 Potential implications for deltaic systems

Whatever the percentage at which the exact transition occurs, it remains true that the existence of a connectivity threshold should be important in natural systems. In the WLD, *Olliver and Edmonds* [2017] estimated that island vegetation coverage is often below 40%-50%, particularly for more distal islands. Temporal variations in vegetative coverage — whether seasonal, yearly, or in response to storms [*Carle et al.*, 2013; *Carle and Sasser*, 2016] — should entail periods of high and low connectivity, particularly if the vegetation population crosses this threshold. In a previous study, *Sendrowski and Passalacqua* [2017] observed a loss in system-scale transfer entropy links between periods of minimum and maximum biomass in the WLD, which may have corresponded to vegetation coverage crossing this disconnectivity threshold, thus restricting the cross-delta transfer of information.

The results of the present study could have implications for the ecogeomorphic succession of deltaic systems. In our model, static vegetation offered a control on flow, but in reality the reverse would also be true. It is possible that, through autogenic processes, vegetation would self-organize towards a particular distribution of patch sizes, coverage, or stem densities that best optimizes their living conditions. Important questions remain regarding whether a stable state (or multiple quasi-stable states) exist for vegetation in deltaic systems, what they would be, and whether they are attainable. Further research is required to determine how vegetation would respond to the hydrodynamic and transport behavior observed here, but the results of the present study could help inform such an analysis.

As is discussed in section 3.2.2, our results from modeling intermediate roughness values ($nh_v = 0.5, 1.0$) reveal a logarithmic decrease in the amount of tracer delivered to the islands for an increase in vegetation density (Figure 3.7). Therefore, there is a trade-off between the ability to deliver sediment and nutrients to the islands and the ability to retain what arrives there. Vegetation and topography could co-evolve to achieve conditions most favorable for vegetation stability, potentially near the disconnectivity threshold as hypothesized in previous studies [*Luhar et al.*, 2008]. Future research is needed to understand precisely how ecogeomorphic feedbacks influence the evolution of coastal deltas.

4.2 The role of patch size

Below the disconnectivity threshold, increasing patch size tends to exacerbate differences between the behavior of patchy and uniform scenarios. Runs with larger patches tend to develop more well-established flow corridors in the islands (Figure 4.2). These flow corridors can lead to large localized hotspots of connectivity when adjacent to the main channel (Figure C.3), which function similarly to established secondary channels in natural systems [*Hiatt and Passalacqua*, 2015]. Interestingly, transects like those shown in Figure C.3 for runs with the largest patch sizes often demonstrate a number of local maxima, indicating that a considerable amount of flow can sometimes be re-routed into the central channel from the islands. This corresponds to scenarios in which the high-velocity channels terminate back at the main channel, with no other optimal route for flow. It has yet to be seen whether similar behavior occurs in natural systems, but if it does, it would likely divide the island into two over time, eventually forming a new bifurcation and downstream confluence. These results therefore demonstrate a potential avenue for vegetation to act as the driving force behind topological changes on the deltaic distributary network.

When patches are small, the critical transition near the threshold of channelization is fairly smooth (e.g. Figure 3.5); as patch sizes increase, however, the transition becomes more step-like. Model results at 25m resolution suggest that this effect is not a result of the numerical model (Table A.1), but is rather an actual trend in the hydraulic behavior of the system. We therefore hypothesize that when patches are large and coverage is low, island transport relies more on bathymetric geometry than vegetation characteristics.

Patches on the order of 50m-100m in diameter are certainly of the scale that we observe in systems like the WLD (see Figure 2.1b), but patches that are 250m in diameter may be bordering on unrealistic — at least for small systems like the WLD. We expect that the observed flow through regions of smaller patches more accurately represents reality, and suggest that any future work which draws upon this analysis give the model runs with the largest patches lower credence in their interpretation of these results.

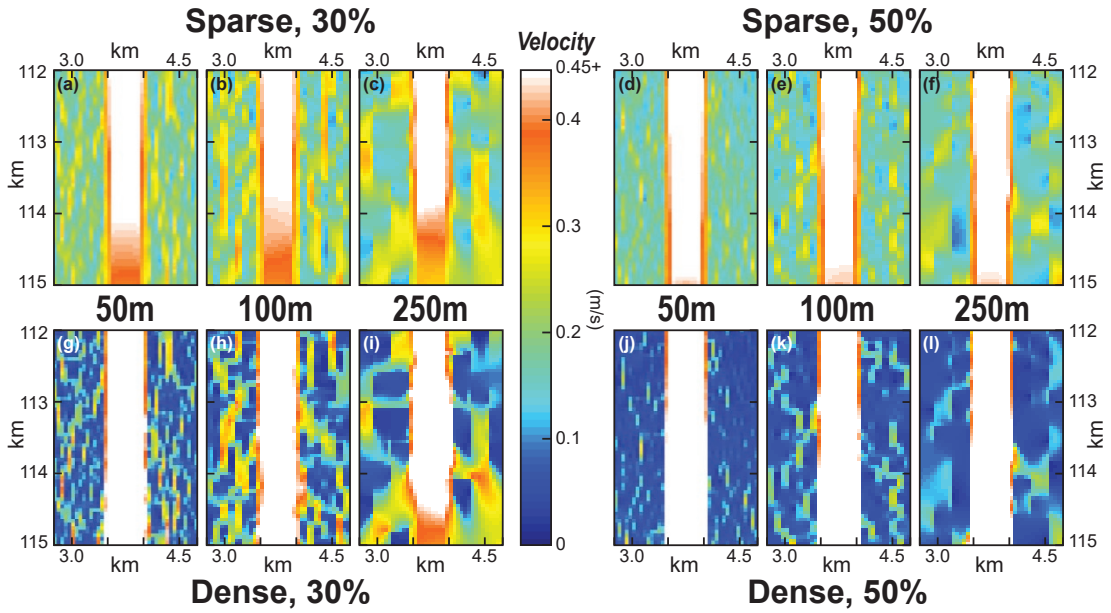

Figure 4.2: The influence of patch size on flow velocity magnitudes throughout a representative section of the CIC for sparse **(a-f)** and dense **(g-l)** vegetation. Shown are maps at 30% (a-c,g-i) and 50% (d-f,h-l) cover for 50m, 100m, and 250m wide patches.

4.3 Implications for the modeling of deltaic systems

While the implications of vegetation heterogeneity on delta hydrodynamics are important, deltaic models often go beyond hydrodynamics to assess the merits of engineering projects intended to promote land growth (e.g. sediment diversions) or improve water quality (e.g. rebuilding wetlands). While the present study exclusively models hydrodynamics, we discuss the potential effects of heterogeneous vegetation on the ability of deltaic models to estimate aggradation and denitrification potential.

Estimating actual locations of aggradation depends on where sediment is routed, which has not been modeled explicitly here — however, it is apparent from the maps of shear velocity (Figure 3.8) that a considerable amount of transport is predicted to occur within the islands when vegetation coverage is below the disconnectivity threshold. Neglecting vegetation heterogeneity in the modeling of

deltaic systems may lead to the erroneous conclusion that the vegetated islands are incapable of transporting the D_{50} grain size under non-flood conditions. It would also underestimate the total amount of flow (and therefore sediment) being delivered to the island interior. Thus, the explicit treatment of vegetation heterogeneity should be included in hydromorphodynamic models of deltas.

It is known that the RTD of a wetland system is an important control parameter for biogeochemical nutrient processing [*Kadlec and Wallace*, 2008; *Cheng and Basu*, 2017]. Because vegetation patchiness alters the shape of the RTD through the CIC (Figures C.1, 3.5, and 3.6), it stands to reason that estimates of nutrient processing would also be affected [*Hiatt et al.*, 2018]. Below the disconnectivity threshold, the RTD for patchy runs differs from the RTD for uniform runs in shape (often multi-modal), temporal behavior (peak often delayed), and in the relative contribution of the islands to the full RTD (sometimes displaying more than a two-fold increase in net island flux). To the extent that the bulk system RTD reflects the degree of biotic nutrient processing, estimates based on patchy model runs may predict higher nutrient retention rates for the delta complex than would estimates based on uniform vegetation. There is, however, a trade-off between the increased island flux in patchy runs and the reduction in RTD due to high-velocity preferential flow-paths. It is possible that short-circuiting due to the high-velocity preferential flow-paths would actually lead to decreases in wetland nutrient processing. Further research is needed to constrain the RTD of deltaic islands with spatially-variable vegetation and its resulting impact on denitrification and the removal of other nutrients in the delta complex.

For full-complexity deltaic models, the range of effects observed in the present study due to heterogeneity ought to be an important consideration. If vegetation is relatively sparse, treating vegetation as homogeneous may be an appropriate approximation. However, if the vegetation is very dense, approximating it as homogeneous within a deltaic island will likely lead to a conservative estimate of channel-island hydrological connectivity and will underestimate the capabilities of flow pathways within the island to form and transport sediment and nutrients to the island interior.

4.4 Limitations

A few limitations of the present study should be noted. First, the random maps of vegetation modeled here are still quite simplified with respect to actual deltaic vegetation. Vegetation colonization is not fully random, but rather influenced by flow conditions and elevation differences in the deltaic marsh. The intention of this study, however, is not to try to accurately represent the full range of possible vegetation found in deltaic marshes, but rather to explore connectivity in a system that is one step in complexity above that of fully uniform vegetation. We believe that uniform random maps provide a good first-order approximation of heterogeneous vegetation. Connecting these results to the hydrogeomorphic processes of natural system remains non-trivial, but the present study gets us closer to the processes of the fully complex system without necessarily losing generality to systems outside the WLD. Future studies should explore more complex vegetated distributions in deltaic settings.

It would be beneficial to have more model initializations in each ensemble over which to average the hydraulic behavior of the system. While five random maps per scenario is not statistically ideal, the long run-time required by each model run made testing additional maps per scenario too computationally intensive. The small variation observed between each set of five initializations, particularly when patch size is small, leads us to conclude that five runs is sufficient to have confidence in the findings presented herein. The phenomena we observe across our model runs — such as the increase in connectivity in patchy runs and the formation of preferential flow-paths at low percent cover — persist throughout each ensemble. However, we caution that any future studies based on these results bear in mind the relatively few numbers of model runs considered for each scenario in this study.

Lastly, the mechanics of flow through vegetation is fairly complex, and our use of the shallow water, Baptist, and Wilcock equations are all simplifying approximations that introduce their own set of errors into this analysis. Surely the turbulent interactions at different levels of patch density could have important implications for the dynamics measured here, as could the 3D flow structures that form atop the neglected submerged vegetation. However, these errors are likely to

be small over the spatial scales measured here. Additionally, the Wilcock equation was not developed for vegetated flows, and it stands to reason that the roughness height z_0 in that equation could noticeably increase in regions of vegetation. However, in our analysis of shear velocities we focus our attention primarily on the non-vegetated regions of the domain in which there is transport, rather than on the vegetated regions in which this equation is perhaps less accurate. Thus, we believe the errors introduced by our use of the Wilcock equation will minimally influence our conclusion that more sediment is capable of transport in much of the deltaic islands when vegetation is heterogeneous.

Chapter 5: Conclusions and future work

In the present work, we used a depth-integrated hydrodynamic model in an idealized channel-island complex to analyze the influence of patchy, heterogeneous vegetation on hydrological connectivity and transport in river deltas. The computational domain is based on the Wax Lake Delta in coastal Louisiana, with deltaic islands populated by randomly distributed vegetation patches of a given size, percent cover, and stem density. These three vegetation characteristics were varied in our model runs, and five random initializations were modeled for each unique pairing of these characteristics to determine the average behavior of each ensemble. Then, using tracer studies, we developed residence time distributions for each model scenario and analyzed the impact of vegetation characteristics on transport through the domain as a proxy for nutrients or sediment.

In section 1.5, we laid out three driving research questions for the present analysis, which may be summarized as such: (1) To what extent does the spatial-variability of deltaic vegetation affect channel-island connectivity? (2) Beyond flow, what are the implications of vegetation heterogeneity on other deltaic processes, such as the transport of solutes or its ecogeomorphic evolution? (3) What does this mean for our ability to effectively model deltaic restoration efforts? We additionally presented three relevant hypotheses — namely, (1) the heterogeneity of vegetation will affect the hydrodynamics of the system, (2) an increase in percent cover and stem density will decrease channel-island connectivity, and (3) the importance of heterogeneity is likely to scale with patch size.

In our modeling analysis, we observe an increase in channel-island hydrological connectivity in model runs in which vegetation is heterogeneous when compared to model runs with the same spatially-averaged roughness applied uniformly throughout the islands. This increase in connectivity is negligible when vegetation is sparse or coverage is high, but it is substantial when vegetation is dense and covers less than a "disconnectivity" threshold of $40\% - 50\%$ of the islands. The disparity between patchy and uniform scenarios is additionally enhanced by an increase in patch size. Below the threshold, we observe (1) an up to 27% increase

in lateral outflow from the central distributary channel into the islands, (2) the formation of high-velocity preferential flow-paths in the islands, which are capable of transporting not only flow but also the median sediment grain size of the WLD, and (3) as much as a factor of two increase in the proportion of a passive tracer that is allocated to the islands. Once this threshold is crossed, the flow field in patchy runs becomes effectively homogeneous, and there is only a minor increase in lateral outflow or the proportion of tracer allocated to the islands, when compared to uniform runs. This disconnectivity threshold is near the theoretical percolation threshold and may demonstrate the effects of percolating flow-paths on hydrodynamics in a vegetated system. We therefore confirm all three of our aforementioned hypotheses, with the caveat that the significance of heterogeneity strongly depends upon vegetation characteristics.

The results of this work suggest that models of deltaic systems – such as those projecting the effects of sediment diversions or other coastal restoration efforts – should consider the possible effects of heterogeneous vegetation on the system being modeled. The increase in connectivity we observe suggests that models which neglect to account for spatial complexity could underestimate channel-island hydrological connectivity, over-estimate the ability for deltaic islands to retain sediment, and underestimate the potential for denitrification and other ambient nutrient processing in the marshes of the deltaic islands. The existence of the observed disconnectivity threshold could have implications beyond hydrodynamics, such as on the long-term ecogeomorphic or biogeochemical evolution of natural deltaic systems.

Appendix A: Discretization tests at 25m resolution

Table A.1: Comparison of cumulative tracer flux for identical runs at 50m and 25m resolution. The average (± standard deviation) tracer flux for patchy runs at 30% and 50% cover are 0.3934 (± 0.0117) and 0.2878 (± 0.0143), respectively.

Scenario	50m Resolution	25m Resolution
30% Cover, Uniform	0.2774	0.2607
30% Cover, Patchy	0.4016	0.4242
50% Cover, Uniform	0.2390	0.2249
50% Cover, Patchy	0.2781	0.2896

Appendix B: Ensemble statistics

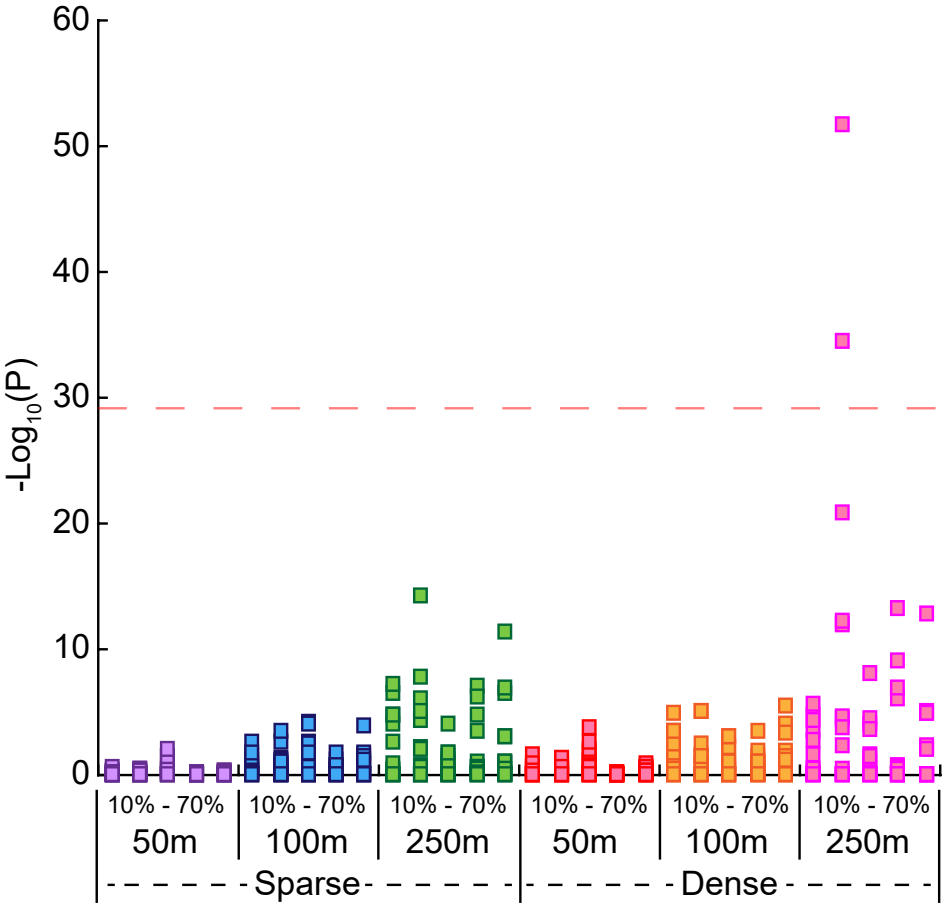

Figure B.1: The statistical similarity of model runs in each ensemble. On the abscissa is each vegetation scenario (each unique pairing of percent cover, patch size, and density). On the ordinate is the negative logarithm of the p value from a Wilcoxon rank-sum comparison of the island velocities in each given model run. For every scenario, each of the five runs is compared to each of the others, for a total of 10 comparisons. Data points which are higher on the ordinate are more statistically dissimilar. The threshold for statistical dissimilarity (the red dashed line) is chosen such that 95% of rank-sum tests comparing model runs with different vegetation characteristics falls above that line. Only one model run (run 4 at 30% cover, 250m patches, dense vegetation) exceeds this threshold.

Appendix C: Supplementary figures

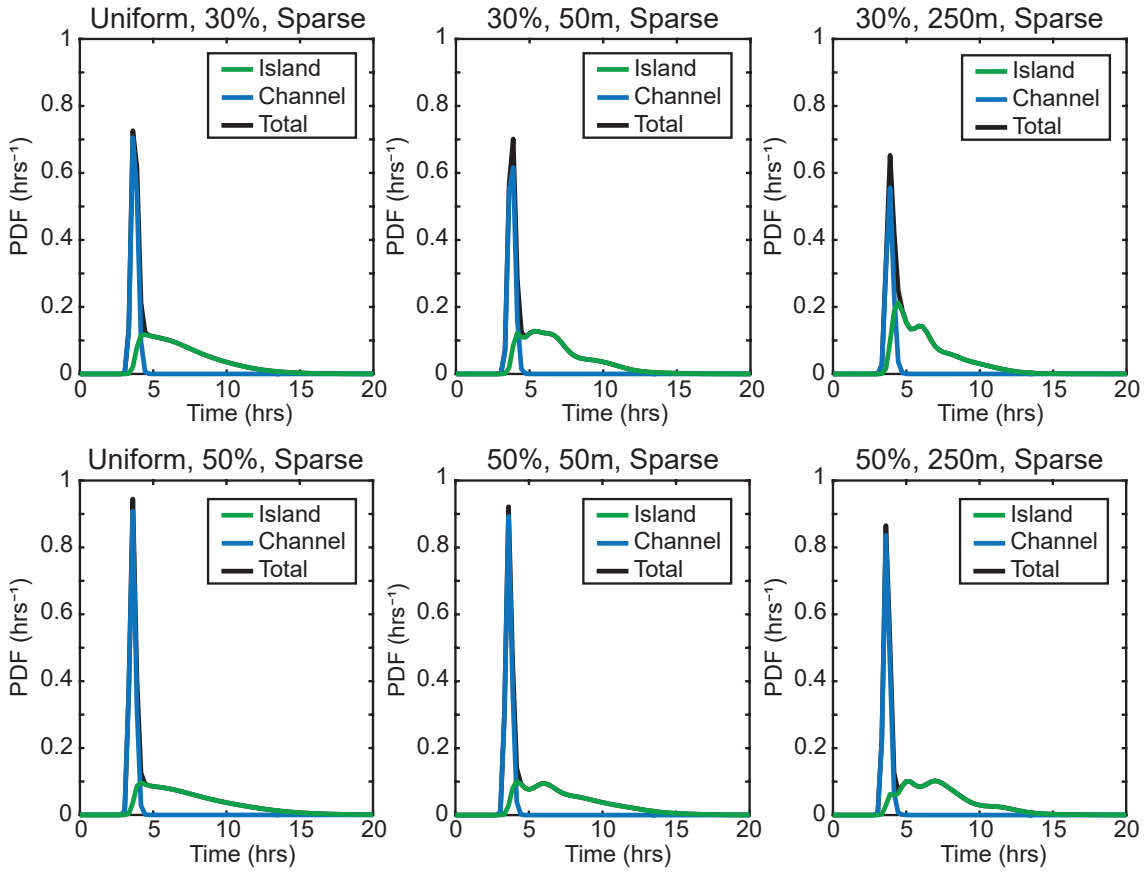

Figure C.1: Example residence time distributions, as well as the decomposition of the RTD into channel and island components. These RTDs correspond to runs at 30% (a-c) and 50% (d-f) coverage, at 50m and 250m patch sizes, and sparse vegetation. Also shown are the results for the corresponding uniform run. The relative size of the channel and island curves is not significantly changed for a change in patch size, but the shape of the island curve is much more variable and multi-modal.

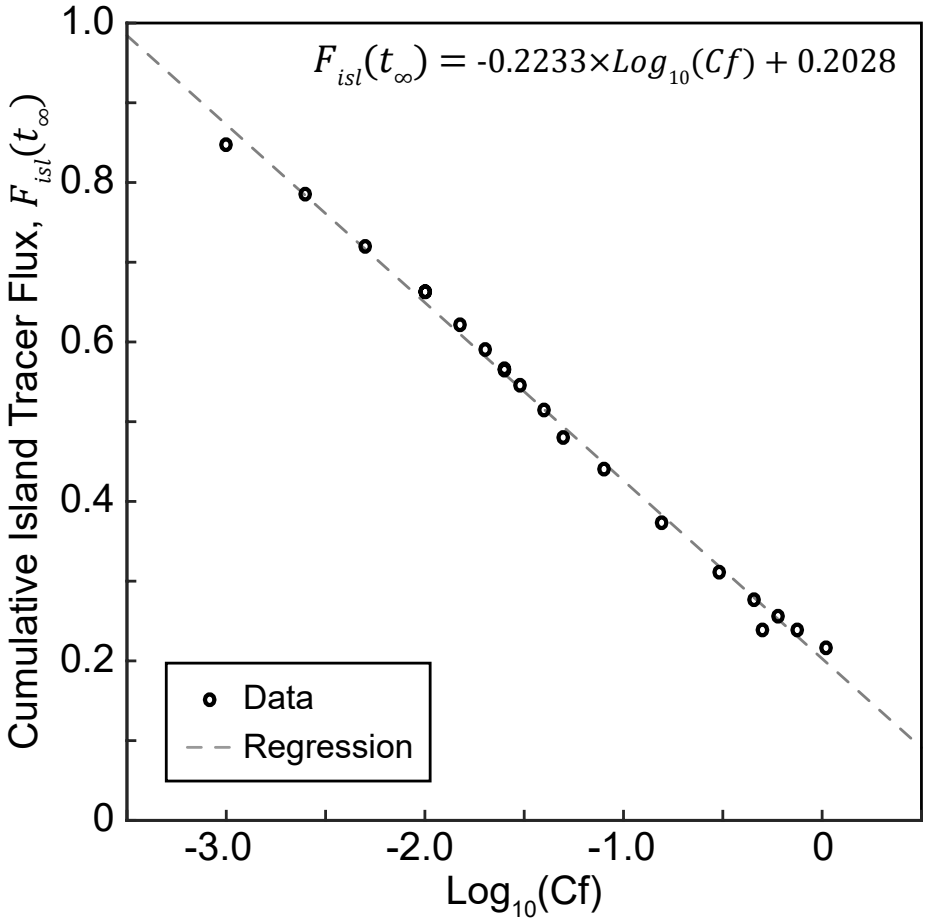

Figure C.2: Cumulative fraction of tracer allocated to the islands for all uniform scenarios vs the logarithm of the island roughness coefficient. The black circles show the modeled data from the present study and *Hiatt and Passalacqua* [2017], and the grey dashed line shows a linear regression. The equation is given in the top right.

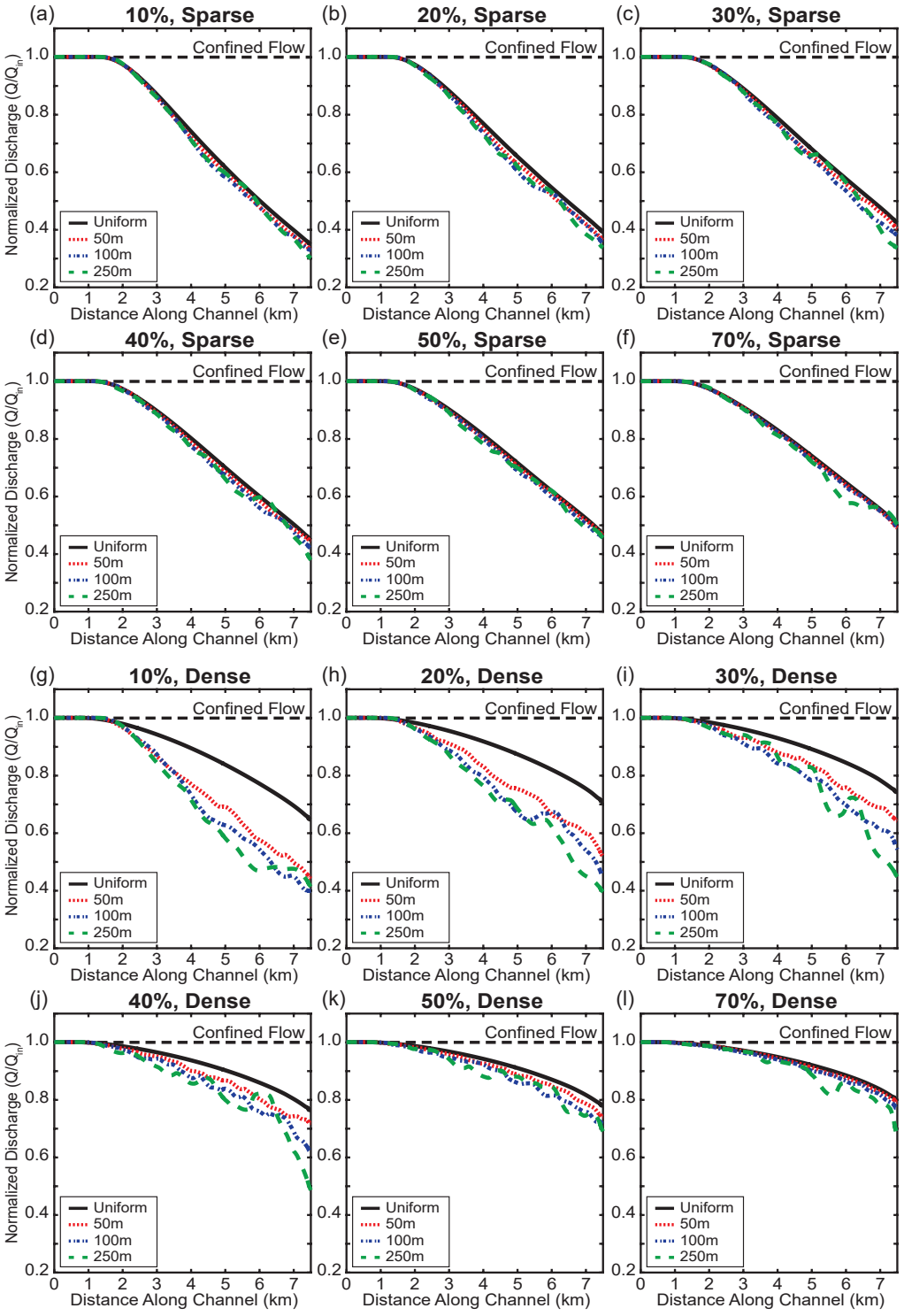

Figure C.3: Discharge transects for the first run in all vegetation coverage scenarios. Select curves are included in the ensembles shown in Figure 3.1.

Appendix D: MATLAB code for map generation

```
%% Island Roughness Distribution=================================
% Script produces a vegetation map of randomly distributed patches
% with a specified percent cover, patch size, and patch roughness
bathy = load('bathy_changeCf_50m_100km_fixed.mat'); % Load bathymetry

% Input Vegetation Characteristics:
Percent_cover = 50; % Changing this value changes percent cover
Patch_size = 1; % Set patch size: {1,2,5}, i.e. {50m,100m,250m}
Veg_cf = 0.055; % Vegetated drag coefficient (Baptist et al., 2007)

Patch_size_2 = Patch_size; % Allows for anisotropic patches
Channel_cf = 0.005; % Default bed drag coefficient
Cf_final = zeros(size(bathy.eta,1),size(bathy.eta,2)) + Channel_cf;

%% Check for Domain Size Error====================================
if (mod(2300,Patch_size)>0)
    error('Domain Size Error');
elseif (mod(60,Patch_size_2)>0)
    error('Domain Size Error');
end
%% Random Patches=================================================
% Only save map within 1% cover of target; Variable to be updated:
QualityCheck = Percent_cover + 10;
while abs(QualityCheck-Percent_cover) > 1
% Populate smaller array with random integers from 1-100:
Island_cf = randi([1 100],2300/Patch_size,60/Patch_size_2);

Island_cf(Island_cf<=Percent_cover) = Veg_cf; % Vegetated cells
Island_cf(Island_cf>Percent_cover) = Channel_cf; % Non-vegetated

% Expand array to island domain size:
Island_cf = repelem(Island_cf,Patch_size,Patch_size_2);
% Fill islands (and surrounding area):
Cf_final(1:2300,10:69) = Island_cf; Cf_final(1:2300,82:141) =
    Island_cf;
% Update QualityCheck (i.e. Actual percent cover)
IslandRegion = [Cf_final(2150:2300,56:69) Cf_final(2150:2300,82:95)];
QualityCheck = sum(sum(IslandRegion==Veg_cf))/numel(IslandRegion)
    *100;
end
save('Cf_50Percent_P1_R5.txt','Cf_final','-ASCII')
```

Bibliography

Addicott, J. F., J. M. Aho, M. F. Antolin, D. K. Padilla, J. S. Richardson, and D. A. Soluk (1987), Ecological neighborhoods: scaling environmental patterns, *Oikos*, pp. 340–346.

Adger, W. N. (1999), Social vulnerability to climate change and extremes in coastal Vietnam, *World development*, *27*(2), 249–269.

Allen, Y. C., B. R. Couvillion, and J. A. Barras (2012), Using multitemporal remote sensing imagery and inundation measures to improve land change estimates in coastal wetlands, *Estuaries and Coasts*, *35*(1), 190–200.

Allison, M. A., C. R. Demas, B. A. Ebersole, B. A. Kleiss, C. D. Little, E. A. Meselhe, N. J. Powell, T. C. Pratt, and B. M. Vosburg (2012), A water and sediment budget for the lower Mississippi–Atchafalaya River in flood years 2008–2010: implications for sediment discharge to the oceans and coastal restoration in Louisiana, *Journal of Hydrology*, *432*, 84–97.

Auerbach, L., S. Goodbred Jr, D. Mondal, C. Wilson, K. Ahmed, K. Roy, M. Steckler, C. Small, J. Gilligan, and B. Ackerly (2015), Flood risk of natural and embanked landscapes on the Ganges-Brahmaputra tidal delta plain, *Nature Climate Change*, *5*(2), 153–157.

Bai, J., R. Xiao, K. Zhang, and H. Gao (2012), Arsenic and heavy metal pollution in wetland soils from tidal freshwater and salt marshes before and after the flow-sediment regulation regime in the Yellow River Delta, China, *Journal of Hydrology*, *450*, 244–253.

Baptist, M., V. Babovic, J. Rodríguez Uthurburu, M. Keijzer, R. Uittenbogaard, A. Mynett, and A. Verwey (2007), On inducing equations for vegetation resistance, *Journal of Hydraulic Research*, *45*(4), 435–450.

Barbier, E. B., I. Y. Georgiou, B. Enchelmeyer, and D. J. Reed (2013), The value of wetlands in protecting southeast Louisiana from hurricane storm surges, *PloS one*, *8*(3), e58,715.

Benjamin, M. M., and D. F. Lawler (2013), *Water quality engineering: Physical/-chemical treatment processes*, John Wiley & Sons.

Carle, M. (2013), Spatial structure and dynamics of the plant communities in a pro-grading river delta: Wax Lake Delta, Atchafalaya Bay, Louisiana, Ph.D. thesis, Louisiana State University.

Carle, M. V., and C. E. Sasser (2016), Productivity and resilience: long-term trends and storm-driven fluctuations in the plant community of the accreting Wax Lake Delta, *Estuaries and coasts*, *39*(2), 406–422.

Carle, M. V., C. E. Sasser, and H. H. Roberts (2013), Accretion and vegetation community change in the Wax Lake Delta following the historic 2011 Mississippi River flood, *Journal of Coastal Research*, *31*(3), 569–587.

Casulli, V., and E. Cattani (1994), Stability, accuracy and efficiency of a semi-implicit method for three-dimensional shallow water flow, *Computers & Mathematics with Applications*, *27*(4), 99–112.

Casulli, V., and R. T. Cheng (1992), Semi-implicit finite difference methods for three-dimensional shallow water flow, *International Journal for numerical methods in fluids*, *15*(6), 629–648.

Cheng, F. Y., and N. B. Basu (2017), Biogeochemical hotspots: Role of small water bodies in landscape nutrient processing, *Water Resources Research*.

Corenblit, D., E. Tabacchi, J. Steiger, and A. M. Gurnell (2007), Reciprocal interactions and adjustments between fluvial landforms and vegetation dynamics in river corridors: a review of complementary approaches, *Earth-Science Reviews*, *84*(1), 56–86.

Couvillion, B. R., J. A. Barras, G. D. Steyer, W. Sleavin, M. Fischer, H. Beck, N. Trahan, B. Griffin, and D. Heckman (2011), Land area change in coastal Louisiana from 1932 to 2010, *Tech. rep.*, U.S. Geological Survey.

CPRA (2017), Integrated ecosystem restoration and hurricane protection: Louisiana's comprehensive master plan for a sustainable coast, *Tech. rep.*, Coastal Protection and Restoration Authority of Louisiana (CPRA), Baton Rouge, LA.

Dagan, G. (1984), Solute transport in heterogeneous porous formations, *Journal of fluid mechanics*, *145*, 151–177.

D'Alpaos, A., and M. Marani (2016), Reading the signatures of biologic–geomorphic feedbacks in salt-marsh landscapes, *Advances in Water Resources*, *93*, 265–275.

D'Alpaos, A., M. Toffolon, and C. Camporeale (2016), Ecogeomorphological feedbacks of water fluxes, sediment transport and vegetation dynamics in rivers and estuaries, *Advances in Water Resources*, *93*, 151–155.

Day, J. W., J. Agboola, Z. Chen, C. DElia, D. L. Forbes, L. Giosan, P. Kemp, C. Kuenzer, R. R. Lane, R. Ramachandran, et al. (2016), Approaches to defining deltaic sustainability in the 21st century, *Estuarine, coastal and shelf science*, *183*, 275–291.

Donner, W., and H. Rodríguez (2008), Population composition, migration and inequality: The influence of demographic changes on disaster risk and vulnerability, *Social forces*, *87*(2), 1089–1114.

Douglas, I., K. Alam, M. Maghenda, Y. Mcdonnell, L. McLean, and J. Campbell (2008), Unjust waters: climate change, flooding and the urban poor in Africa, *Environment and urbanization*, *20*(1), 187–205.

Follett, E. M., and H. M. Nepf (2012), Sediment patterns near a model patch of reedy emergent vegetation, *Geomorphology*, *179*, 141–151.

Fonseca, M. S., and S. S. Bell (1998), Influence of physical setting on seagrass landscapes near Beaufort, North Carolina, USA, *Marine Ecology Progress Series*, pp. 109–121.

Freeze, R. A. (1975), A stochastic-conceptual analysis of one-dimensional groundwater flow in nonuniform homogeneous media, *Water Resources Research*, *11*(5), 725–741.

Giosan, L. (2014), Protect the world's deltas, *Nature*, *516*(7529), 31.

Grinsted, A., J. C. Moore, and S. Jevrejeva (2010), Reconstructing sea level from paleo and projected temperatures 200 to 2100 AD, *Climate Dynamics*, *34*(4), 461–472.

Gustafson, E. J., and G. R. Parker (1992), Relationships between landcover proportion and indices of landscape spatial pattern, *Landscape ecology*, *7*(2), 101–110.

Hiatt, M., and P. Passalacqua (2015), Hydrological connectivity in river deltas: The first-order importance of channel-island exchange, *Water Resources Research*, *51*(4), 2264–2282.

Hiatt, M., and P. Passalacqua (2017), What Controls the Transition from Confined to Unconfined Flow? Analysis of Hydraulics in a Coastal River Delta, *Journal of Hydraulic Engineering*, *143*(6).

Hiatt, M., E. Castañeda-Moya, R. Twilley, B. R. Hodges, and P. Passalacqua (2018), Channel-island connectivity affects water exposure time distributions in a coastal river delta, *Water Resources Research*, *54*(0), doi:10.1002/2017WR021289.

Hirabayashi, Y., R. Mahendran, S. Koirala, L. Konoshima, D. Yamazaki, S. Watanabe, H. Kim, and S. Kanae (2013), Global flood risk under climate change, *Nature Climate Change*, *3*(9), 816–821.

Hodges, B. R. (2004), Accuracy order of Crank–Nicolson discretization for hydrostatic free-surface flow, *Journal of engineering mechanics*, *130*(8), 904–910.

Hodges, B. R. (2014), A new approach to the local time stepping problem for scalar transport, *Ocean Modelling*, *77*, 1–19.

Hodges, B. R., and F. J. Rueda (2008), Semi-implicit two-level predictor–corrector methods for non-linearly coupled, hydrostatic, barotropic/baroclinic flows, *International Journal of Computational Fluid Dynamics*, *22*(9), 593–607.

Hodges, B. R., J. Imberger, A. Saggio, and K. B. Winters (2000), Modeling basin-scale internal waves in a stratified lake, *Limnology and oceanography*, *45*(7), 1603–1620.

Hunt, A. G., and M. Sahimi (2017), Flow, transport, and reaction in porous media: Percolation scaling, critical-path analysis, and effective medium approximation, *Reviews of Geophysics*.

Kadlec, R. H., and S. Wallace (2008), *Treatment wetlands*, CRC press.

Khan, M. R., M. Koneshloo, P. S. Knappett, K. M. Ahmed, B. C. Bostick, B. J. Mailloux, R. H. Mozumder, A. Zahid, C. F. Harvey, A. Van Geen, et al. (2016), Megacity pumping and preferential flow threaten groundwater quality, *Nature communications*, *7*, 12,833.

Kim, W., D. Mohrig, R. Twilley, C. Paola, and G. Parker (2009b), Is it feasible to build new land in the Mississippi River Delta?, *EOS, Transactions American Geophysical Union*, *90*(42), 373–374.

Kingsford, R. T. (2000), Ecological impacts of dams, water diversions and river management on floodplain wetlands in Australia, *Austral Ecology*, *25*(2), 109–127.

Knutson, T. R., J. L. McBride, J. Chan, K. Emanuel, G. Holland, C. Landsea, I. Held, J. P. Kossin, A. Srivastava, and M. Sugi (2010), Tropical cyclones and climate change, *Nature Geoscience*, *3*(3), 157–163.

Lane, R. R., J. W. Day Jr, B. D. Marx, E. Reyes, E. Hyfield, and J. N. Day (2007), The effects of riverine discharge on temperature, salinity, suspended sediment and chlorophyll a in a Mississippi delta estuary measured using a flow-through system, *Estuarine, Coastal and Shelf Science*, *74*(1-2), 145–154.

Larsen, L. G., and J. W. Harvey (2010), How vegetation and sediment transport feedbacks drive landscape change in the everglades and wetlands worldwide, *The American Naturalist*, *176*(3), E66–E79.

Larsen, L. G., and J. W. Harvey (2011), Modeling of hydroecological feedbacks predicts distinct classes of landscape pattern, process, and restoration potential in shallow aquatic ecosystems, *Geomorphology*, *126*(3), 279–296.

Larsen, L. G., J. Ma, and D. Kaplan (2017), How important is connectivity for surface water fluxes? a generalized expression for flow through heterogeneous landscapes, *Geophysical Research Letters*, 2017GL075432.

Leauthaud, C., S. Duvail, O. Hamerlynck, J.-L. Paul, H. Cochet, J. Nyunja, J. Albergel, and O. Grünberger (2013), Floods and livelihoods: The impact of changing water resources on wetland agro-ecological production systems in the Tana River Delta, Kenya, *Global Environmental Change*, *23*(1), 252–263.

Leonardi, N., I. Carnacina, C. Donatelli, N. K. Ganju, A. J. Plater, M. Schuerch, and S. Temmerman (2017), Dynamic interactions between coastal storms and salt marshes: A review, *Geomorphology*.

Li, S., H. Shi, Z. Xiong, W. Huai, and N. Cheng (2015), New formulation for the effective relative roughness height of open channel flows with submerged vegetation, *Advances in Water Resources*, *86*, 46–57.

Li, X., C. Liang, and J. Shi (2012), Developing wetland restoration scenarios and modeling its ecological consequences in the Liaohe river delta wetlands, China, *CLEAN–Soil, Air, Water*, *40*(10), 1185–1196.

Liang, M., V. Voller, and C. Paola (2015), A reduced-complexity model for river delta formation–part 1: Modeling deltas with channel dynamics, *Earth Surface Dynamics*, *3*(1), 67–86.

Luhar, M., and H. M. Nepf (2013), From the blade scale to the reach scale: A characterization of aquatic vegetative drag, *Advances in Water Resources*, *51*, 305–316.

Luhar, M., J. Rominger, and H. Nepf (2008), Interaction between flow, transport and vegetation spatial structure, *Environmental Fluid Mechanics*, *8*(5-6), 423.

McGranahan, G., D. Balk, and B. Anderson (2007), The rising tide: assessing the risks of climate change and human settlements in low elevation coastal zones, *Environment and urbanization*, *19*(1), 17–37.

Meire, D. W., J. M. Kondziolka, and H. M. Nepf (2014), Interaction between neighboring vegetation patches: Impact on flow and deposition, *Water Resources Research*, *50*(5), 3809–3825.

Mendelssohn, I. A., G. L. Andersen, D. M. Baltz, R. H. Caffey, K. R. Carman, J. W. Fleeger, S. B. Joye, Q. Lin, E. Maltby, E. B. Overton, et al. (2012), Oil impacts on coastal wetlands: implications for the Mississippi River Delta ecosystem after the Deepwater Horizon oil spill, *BioScience*, *62*(6), 562–574.

Meselhe, E., J. A. McCorquodale, J. Shelden, M. Dortch, T. S. Brown, P. Elkan, M. D. Rodrigue, J. K. Schindler, and Z. Wang (2013), Ecohydrology component of Louisiana's 2012 Coastal Master Plan: mass-balance compartment model, *Journal of Coastal Research*, *67*(sp1), 16–28.

Meselhe, E. A., I. Georgiou, M. A. Allison, and J. A. McCorquodale (2012), Numerical modeling of hydrodynamics and sediment transport in lower Mississippi at a proposed delta building diversion, *Journal of hydrology*, *472*, 340–354.

Michael, H. A., and C. I. Voss (2008), Evaluation of the sustainability of deep groundwater as an arsenic-safe resource in the bengal basin, *Proceedings of the National Academy of Sciences*, *105*(25), 8531–8536.

Michot, B., E. Meselhe, K. W. Krauss, S. Shrestha, A. S. From, and E. Patino (2015), Hydrologic modeling in a marsh–mangrove ecotone: predicting wetland surface water and salinity response to restoration in the Ten Thousand Islands region of Florida, USA, *Journal of Hydrologic Engineering*, *22*(1), D4015,002.

Mitsch, W. J., J. W. Day Jr, J. W. Gilliam, P. M. Groffman, D. L. Hey, G. W. Randall, and N. Wang (2001), Reducing nitrogen loading to the Gulf of Mexico

from the Mississippi River basin: Strategies to counter a persistent ecological problem, *BioScience*, *51*(5), 373–388.

Mitsch, W. J., J. W. Day, L. Zhang, and R. R. Lane (2005), Nitrate-nitrogen retention in wetlands in the Mississippi River Basin, *Ecological engineering*, *24*(4), 267–278.

Morton, R. A., J. C. Bernier, J. A. Barras, and N. F. Ferina (2005), Historical subsidence and wetland loss in the Mississippi Delta plain, *Gulf Coast Association of Geological Societies Transactions*.

Nardin, W., D. Edmonds, and S. Fagherazzi (2016), Influence of vegetation on spatial patterns of sediment deposition in deltaic islands during flood, *Advances in Water Resources*, *93*, 236–248.

Nepf, H. M. (2012a), Hydrodynamics of vegetated channels, *Journal of Hydraulic Research*, *50*(3), 262–279.

Nepf, H. M. (2012b), Flow and transport in regions with aquatic vegetation, *Annual Review of Fluid Mechanics*, *44*, 123–142.

Nicholls, R. J., and A. Cazenave (2010), Sea-level rise and its impact on coastal zones, *science*, *328*(5985), 1517–1520.

Nittrouer, J. A., and E. Viparelli (2014), Sand as a stable and sustainable resource for nourishing the Mississippi River delta, *Nature Geoscience*, *7*(5), 350.

NOAA (2017), Barataria Basin, `http://gulfspillrestoration.noaa.gov`, Accessed: 2017-09-28.

Oborny, B., G. Szabó, and G. Meszéna (2007), Survival of species in patchy landscapes: percolation in space and time, *Scaling biodiversity. Cambridge University Press, Cambridge*, pp. 409–440.

Olliver, E. A., and D. A. Edmonds (2017), Defining the ecogeomorphic succession of land building for freshwater, intertidal wetlands in Wax Lake Delta, Louisiana, *Estuarine, Coastal and Shelf Science*.

Ortiz, A. C., A. Ashton, and H. Nepf (2013), Mean and turbulent velocity fields near rigid and flexible plants and the implications for deposition, *Journal of Geophysical Research: Earth Surface*, *118*(4), 2585–2599.

Paola, C., R. R. Twilley, D. A. Edmonds, W. Kim, D. Mohrig, G. Parker, E. Viparelli, and V. R. Voller (2011), Natural processes in delta restoration: Application to the Mississippi Delta, *Annual Review of Marine Science*, *3*, 67–91.

Passalacqua, P. (2017), The Delta Connectome: A network-based framework for studying connectivity in river deltas, *Geomorphology*, *277*, 50–62.

Rivera-Monroy, V. H., B. Branoff, E. Meselhe, A. McCorquodale, M. Dortch, G. D. Steyer, J. Visser, and H. Wang (2013), Landscape-level estimation of nitrogen removal in coastal Louisiana wetlands: Potential sinks under different restoration scenarios, *Journal of Coastal Research*, *67*(sp1), 75–87.

Schmitt, K., T. Albers, T. Pham, and S. Dinh (2013), Site-specific and integrated adaptation to climate change in the coastal mangrove zone of Soc Trang Province, Viet Nam, *Journal of Coastal Conservation*, *17*(3), 545–558.

Sendrowski, A., and P. Passalacqua (2017), Process connectivity in a naturally prograding river delta, *Water Resources Research*, *53*.

Shaw, J. B., and D. Mohrig (2014), The importance of erosion in distributary channel network growth, Wax Lake Delta, Louisiana, USA, *Geology*, *42*(1), 31–34.

Shaw, J. B., D. Mohrig, and S. K. Whitman (2013), The morphology and evolution of channels on the Wax Lake Delta, Louisiana, USA, *Journal of Geophysical Research: Earth Surface*, *118*(3), 1562–1584.

Shaw, J. B., F. Ayoub, C. E. Jones, M. P. Lamb, B. Holt, R. W. Wagner, T. S. Coffey, J. A. Chadwick, and D. Mohrig (2016a), Airborne radar imaging of subaqueous channel evolution in Wax Lake Delta, Louisiana, USA, *Geophysical Research Letters*, *43*(10), 5035–5042.

Shaw, J. B., D. Mohrig, and R. W. Wagner (2016b), Flow patterns and morphology of a prograding river delta, *Journal of Geophysical Research: Earth Surface*, *121*(2), 372–391.

Shepard, C. C., C. M. Crain, and M. W. Beck (2011), The protective role of coastal marshes: a systematic review and meta-analysis, *PloS one*, *6*(11), e27,374.

Shields, M. R., T. S. Bianchi, D. Mohrig, J. A. Hutchings, W. F. Kenney, A. S. Kolker, and J. H. Curtis (2017), Carbon storage in the Mississippi River delta enhanced by environmental engineering, *Nature Geoscience*, *10*(11), 846.

Smith, R. W., T. S. Bianchi, M. Allison, C. Savage, and V. Galy (2015), High rates of organic carbon burial in fjord sediments globally, *Nature Geoscience*, *8*(6), 450–453.

Stauffer, D. (1979), Scaling theory of percolation clusters, *Physics reports*, *54*(1), 1–74.

Stelling, G., and M. Zijlema (2003), An accurate and efficient finite-difference algorithm for non-hydrostatic free-surface flow with application to wave propagation, *International Journal for Numerical Methods in Fluids*, *43*(1), 1–23.

Syvitski, J. P., C. J. Vörösmarty, A. J. Kettner, and P. Green (2005), Impact of humans on the flux of terrestrial sediment to the global coastal ocean, *Science*, *308*(5720), 376–380.

Syvitski, J. P., A. J. Kettner, I. Overeem, E. W. Hutton, M. T. Hannon, G. R. Brakenridge, J. Day, C. Vörösmarty, Y. Saito, L. Giosan, et al. (2009), Sinking deltas due to human activities, *Nature Geoscience*, *2*(10), 681.

Tejedor, A., A. Longjas, I. Zaliapin, and E. Foufoula-Georgiou (2015a), Delta channel networks: 1. A graph-theoretic approach for studying connectivity and steady state transport on deltaic surfaces, *Water Resources Research*, *51*(6), 3998–4018.

Tejedor, A., A. Longjas, I. Zaliapin, and E. Foufoula-Georgiou (2015b), Delta channel networks: 2. Metrics of topologic and dynamic complexity for delta

comparison, physical inference, and vulnerability assessment, *Water Resources Research*, *51*(6), 4019–4045.

Tejedor, A., A. Longjas, R. Caldwell, D. A. Edmonds, I. Zaliapin, and E. Foufoula-Georgiou (2016), Quantifying the signature of sediment composition on the topologic and dynamic complexity of river delta channel networks and inferences toward delta classification, *Geophysical Research Letters*, *43*(7), 3280–3287.

Temmerman, S., and M. L. Kirwan (2015), Building land with a rising sea, *Science*, *349*(6248), 588–589.

Temmerman, S., P. Meire, T. J. Bouma, P. M. Herman, T. Ysebaert, and H. J. De Vriend (2013), Ecosystem-based coastal defence in the face of global change, *Nature*, *504*(7478), 79.

Tessler, Z., C. J. Vörösmarty, M. Grossberg, I. Gladkova, H. Aizenman, J. Syvitski, and E. Foufoula-Georgiou (2015), Profiling risk and sustainability in coastal deltas of the world, *Science*, *349*(6248), 638–643.

Tessler, Z. D., C. J. Vörösmarty, I. Overeem, and J. P. Syvitski (2017), A model of water and sediment balance as determinants of relative sea level rise in contemporary and future deltas, *Geomorphology*.

Turner, R. K., D. Burgess, D. Hadley, E. Coombes, and N. Jackson (2007), A cost–benefit appraisal of coastal managed realignment policy, *Global Environmental Change*, *17*(3), 397–407.

Van Oyen, T., L. Carniello, A. D'Alpaos, S. Temmerman, P. Troch, and S. Lanzoni (2014), An approximate solution to the flow field on vegetated intertidal platforms: Applicability and limitations, *Journal of Geophysical Research: Earth Surface*, *119*(8), 1682–1703.

Vandenbruwaene, W., S. Temmerman, T. Bouma, P. Klaassen, M. De Vries, D. Callaghan, P. Van Steeg, F. Dekker, L. Van Duren, E. Martini, et al. (2011), Flow interaction with dynamic vegetation patches: Implications for biogeomorphic evolution of a tidal landscape, *Journal of Geophysical Research: Earth Surface*, *116*(F1).

Vörösmarty, C. J., J. Syvitski, J. Day, A. De Sherbinin, L. Giosan, and C. Paola (2009), Battling to save the worlds river deltas, *Bulletin of the Atomic Scientists*, *65*(2), 31–43.

Wagner, W., D. Lague, D. Mohrig, P. Passalacqua, J. Shaw, and K. Moffett (2017), Elevation change and stability on a prograding delta, *Geophysical Research Letters*, *44*(4), 1786–1794.

Wamsley, T. V., M. A. Cialone, J. M. Smith, J. H. Atkinson, and J. D. Rosati (2010), The potential of wetlands in reducing storm surge, *Ocean Engineering*, *37*(1), 59–68.

Wang, H., G. D. Steyer, B. R. Couvillion, J. M. Rybczyk, H. J. Beck, W. J. Sleavin, E. A. Meselhe, M. A. Allison, R. G. Boustany, C. J. Fischenich, et al. (2014), Forecasting landscape effects of Mississippi River diversions on elevation and accretion in Louisiana deltaic wetlands under future environmental uncertainty scenarios, *Estuarine, Coastal and Shelf Science*, *138*, 57–68.

Wilcock, P. R. (1996), Estimating local bed shear stress from velocity observations, *Water Resources Research*, *32*(11), 3361–3366.

Xing, F., J. Syvitski, A. Kettner, E. Meselhe, J. Atkinson, and A. Khadka (2017), Morphological responses of the Wax Lake Delta, Louisiana, to Hurricanes Rita, *Elem Sci Anth*, *5*.

Yuill, B. T., A. K. Khadka, J. Pereira, M. A. Allison, and E. A. Meselhe (2016), Morphodynamics of the erosional phase of crevasse-splay evolution and implications for river sediment diversion function, *Geomorphology*, *259*, 12–29.

Zhang, W., H. Feng, J. Zheng, A. Hoitink, M. Van Der Vegt, Y. Zhu, and H. Cai (2012), Numerical simulation and analysis of saltwater intrusion lengths in the Pearl River Delta, China, *Journal of Coastal Research*, *29*(2), 372–382.